5-2014

Detailed Analysis of the Domains of Mtr4 and How They Regulate Helicase Activity

Lacy Leigh Taylor
Utah State University

DETAILED ANALYSIS OF THE DOMAINS OF MTR4 AND HOW THEY REGULATE HELICASE ACTIVITY

by

Lacy Taylor

A thesis submitted in partial fulfillment
of the requirements for the degree

of

MASTER OF SCIENCE

in

Biochemistry

Approved:

Dr. Sean J Johnson Major Professor	Dr. Lance C. Seefeldt Committee Member
Dr. Joan M. Hevel Committee Member	Dr. Mark McLellan Vice President for Research and Dean of the School of Graduate Studies

UTAH STATE UNIVERSITY
Logan, Utah

2014

ABSTRACT

Detailed Analysis of the Domains of Mtr4 and

How They Regulate Helicase Activity

by

Lacy L. Taylor, Master of Science

Utah State University, 2014

Major Professor: Dr. Sean J. Johnson
Department: Chemistry and Biochemistry

There are numerous RNAs transcribed in the cell that are not directly involved in protein translation. Maintaining proper levels of RNA is crucial for cell viability, making RNA surveillance an essential process (equivalent to regulating protein levels). Mtr4 is an essential RNA helicase that activates exosome-mediated 3'-5' turnover in RNA processing mechanisms. Mtr4 has several binding partners, with the most prominent one being the complex Trf4/5-Air1/2-Mtr4 polyadenylating (TRAMP) complex. The polyadenylation and unwinding activity of TRAMP is modulated by a sensing mechanism in Mtr4 that detects both length and identity of 3'-end poly(A) tails. While it has been known that Mtr4 has an unwinding preference for substrates with a 3' poly(A) tail and a length of approximately 5 nucleotides, the mechanistic detail is unclear. It is also unclear what structural features of Mtr4 contribute to this sensing function. By using x-ray crystal structures of Mtr4, a ratchet helix was identified to interact with RNA substrates. Significant conservation of this ratchet helix along the RNA binding path was observed, similar to conservation patterns throughout Ski2-like and DEAH/RHA-box helicases.

Structural characterization revealed a novel arch domain shown to bind structured RNAs, which may aid in cooperative RNA recognition in conjunction with the ratchet helix. In this thesis we demonstrate that the conserved residues at the third (R1030) and fourth (E1033) turns of the Mtr4 ratchet helix uniquely influence RNA unwinding rates. Furthermore, when mutated, ratchet helix positions confer slow growth phenotypes to *Saccharomyces cerevisiae* and are synthetically lethal in an Mtr4-archless background. The unwinding activity of these mutants when in the TRAMP complex alters the unwinding rates of Mtr4, and in some instances recovers substrate specificity. Our findings demonstrate the importance of R1030 and E1033 for helicase activity, and additionally link the arch domain of Mtr4 in essential unwinding events.

(79 pages)

PUBLIC ABSTRACT

Detailed Analysis of the Domains of Mtr4 and How They Regulate Helicase Activity

The central dogma states that DNA is transcribed into RNA, which is then translated into protein. This concept conveys a minimal view of the role of RNA, portraying it simply as an intermediary between DNA and protein. However, it is now known that the role of RNA in the cell is critical in regulating protein expression both directly and indirectly. RNA in the cell typically goes through modifications to become active (on) and inactive (off) to eventually become targeted for degradation and start the cycle all over again. The protein complex that regulates the proper maturation and degradation of RNA in the cell is the 3'-5' RNA degrading exosome complex, composed of 9 subunits and several other associating proteins. One such associating protein that helps activate the exosome is the RNA helicase Mtr4.

Mtr4 unwinds structured RNA to then feed the single-stranded RNA through the exosome for proper trimming or degradation. Mtr4 is an essential protein for cell viability, and if functioning improperly, can result in certain neurological and immune disorders. Understanding how Mtr4 works is important to regulating RNA surveillance and treating the diseases and disorders caused by the presence of improperly functioning protein. In this thesis, a detailed analysis of Mtr4 unwinding and substrate recognition is explored. Additionally, our data show an interesting result in which we have discovered a potential role for the novel arch domain of Mtr4.

Lacy L. Taylor

ACKNOWLEDGMENTS

I would like to acknowledge and thank my amazing parents, Gary and Sara, for without whom I would not be where I am today. Their support and encouragement have helped me build strength throughout my journey. I would also like to thank my sisters, Lindsay and Kelly, for their occasional pick-me-up visits out to Utah. I would like to thank my committee members, Dr. Joanie Hevel and Dr. Lance Seefeldt, for their time and patience with me. To my lab members, I would like to thank them for being there and sharing in the roller coaster of emotions that we all experienced through research. Specifically I would like to thank Megi Rexhepaj, Jeremy Bakelar, Stephen Bux, Russell Butler, Lindsey Lott, and Ryan Jackson for his mentorship. Last, but certainly not least, I would like to give big thanks to Dr. Sean Johnson. I could not have asked for a better mentor and principal investigator, who I know, will always have my back.

Lacy L. Taylor

CONTENTS

LIST OF TABLES

LIST OF FIGURES

CHAPTER 1

INTRODUCTION

INTRODUCTORY BACKGROUND AND SIGNIFICANCE

RNA is a multifunctional macromolecule that can store genetic information and catalyze chemical reactions. Several different RNA transcripts are produced in the cell to regulate major pathways such as transcription and translation[1-3] (outlined in Figure 1-1). Almost all RNAs, whether they are involved in storing genetic information or catalyzing reactions, must first undergo modifications to be fully functional. RNA modifications encompass a wide scope of processes, such as splicing, 5'-capping, 3'-polyadenylation, covalent modifications (methylation, etc.), internal cleavage, and end trimming.[4,5]

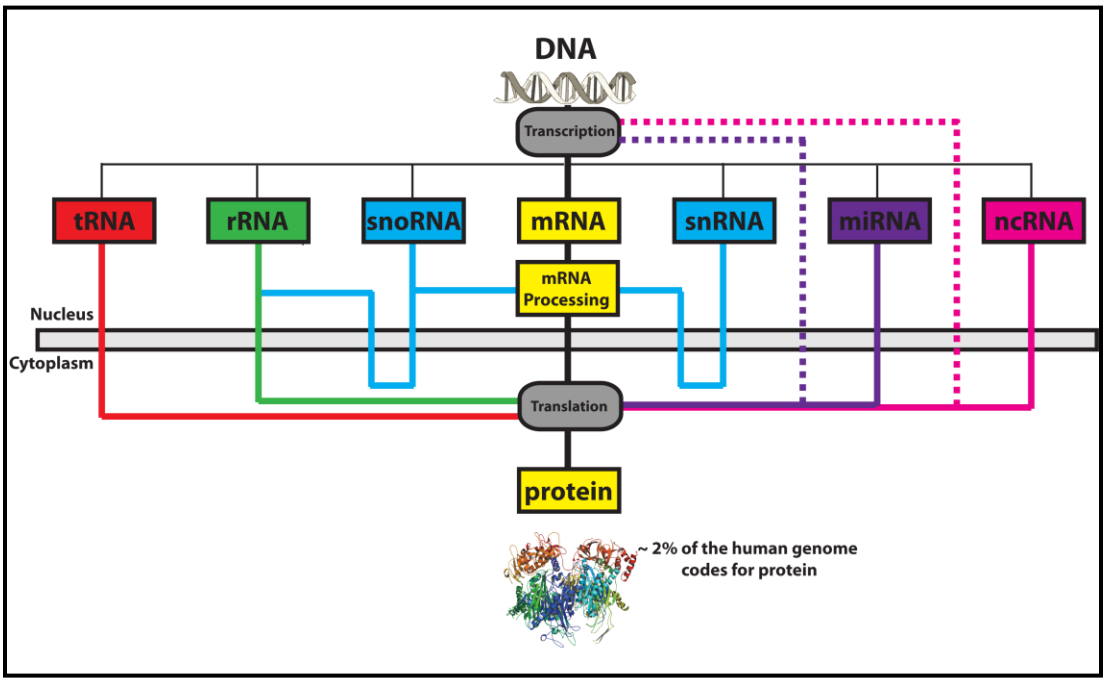

Figure 1-1. Diagram of the cycle of RNA modifications. This diagram emphasizes the importance of regulating RNA levels in the cell.

It is imperative that all RNAs are therefore matured and functioning properly for survival of the cell. It is of equal importance for any improperly transcribed or aberrant

RNAs to be recognized and degraded. The primary complex responsible for the degradation and maturation of various RNAs in eukaryotes (such as rRNA, tRNA, sn(o)RNA, pre-mRNA, cryptic unstable transcripts (CUTs), etc.) is the exosome[6-9]. Certain diseases have been linked to an improperly functioning exosome such as polymyositis/scleroderma-overlap syndrome (PM/Scl) where patients lose muscle[10]. The exosome is crucial for maintaining proper functioning levels of RNA.

The RNA Degradation Machinery

The exosome, which is found in the nucleus and cytoplasm of eukaryotic and archaeal cells, is a multi-subunit complex responsible for 3'-5' degradation of aberrant RNAs in the cell. First discovered in yeast, it was later discovered to have a homologous version in humans. The exosome is comprised of six core RNase PH exoribonucleases (Rrp41, Rrp42, Rrp46, Rrp43, Rrp45, and Mtr3) and three S1/KH proteins (Csl4, Rrp4, and Rrp40) called the capping proteins, that encompass a ring like structure with a gap in the center large enough to accomodate single stranded RNA.[11] Surprisingly, this complex is catalytically inactive without certain cofactors/activators.[10] The exosome functions in a cooperative manner in RNA surveillance with the associated nucleases Rrp6, a 3'-5' exoribonuclease found primarily in the nucleus, and Rrp44 a 3'-5' exo- and endoribonuclease found in the nucleus and cytoplasm.[12]

Rrp44 can degrade structured RNA's, however it has an active site that only allows single stranded RNA. Rrp44 is also considered a 3'-5' RNA helicase that translocates along nucleic acid through the energy release given off by hydrolysis of the RNA substrate.[13] Rrp6 is an exoribonuclease exclusively, that typically degrades non-structured RNA. However, given a 5-10 nucleotide extension on the 3' end, and approximately a 10 nucleotide extension on the 5' end, Rrp6 can degrade through structured portions of RNA.[14] Rrp6 is important for recruiting other activators of the exosome such as Rrp47 and the TRAMP complex,

composed of Trf4/5, Air1/2, and Mtr4.[15-18] The exosome requires these associated nucleases and cofactors/activators to function in RNA surveillance, Figure 1-2.

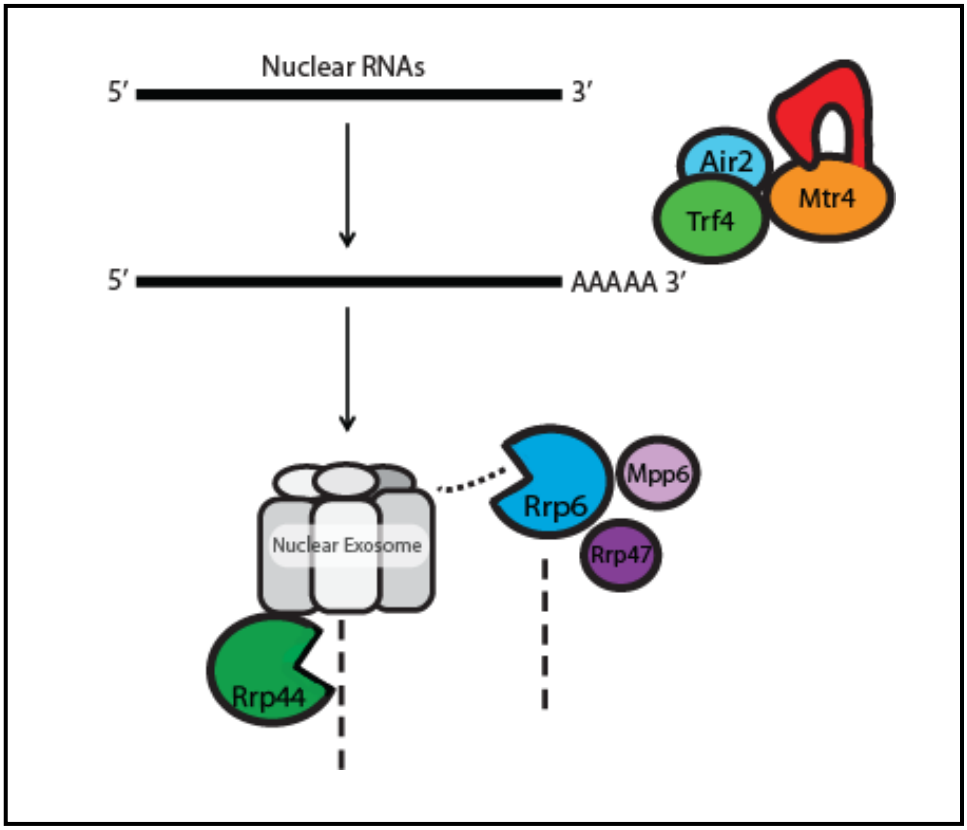

Figure 1-2. Pathway to RNA degradation/maturation. The major degradation machinery, the exosome, and required activators/cofactors.

The RNA Helicase Mtr4

Mtr4 is an essential ATP-dependent RNA helicase that catalyzes the unwinding of structured RNAs and is important for exosome activation.[19] Mtr4 unwinds double-stranded RNA in a 3'-5' direction, and binds single stranded RNA (ssRNA) with a preference for a short poly(A) tail.[20] It is a member of the Ski2-like, DExH-box helicases from superfamily 2 (SF2). There are 6 classifications of superfamily helicases based on their helicase motif type. The term DExH-box helicase is similar to the DEAD-box helicase which is named for a

conserved sequence within motif II (ATPase region) of Asp-Glu-Ala-Asp, with DExH being a variation in this sequence.[21] The DE residues in motif II of these helicases are involved in coordinating a magnesium ion and catalytic water for hydrolysis of ATP.

Each helicase contains a common core structure comprised of two RecA-like domains, a winged helix domain, and a 7-8 helix bundle domain,[22] outlined for Mtr4 in Figure 1-3. RecA-like domains are involved in binding nucleic acids and hydrolyzing ATP and are so named due to their similarity in structure with the ATPase RecA protein involved in DNA recombination.[23] RecA-like folds consist of a central β–sheet followed by α-helices, with a highly conserved sequence motif of A/GXXXXGKT/S between the end of the β1-strand and the flanking α–helix.[23] This sequence motif is involved in coordination of the γ–phosphate of ATP during the hydrolysis reaction.[23]

Following the two RecA-like domains is a winged helix, domain 3. Winged helix domains were originally identified to be involved in nucleic acid binding, however in the case of the replication protein RPA32 it is required for protein-protein interactions.[24] Analysis of the Hel308 structure, which is also a Ski2-like SF2 helicase, shows the winged helix appears to play a minimal role at best at interacting with nucleic acids. It has been proposed that the winged helix in Hel308, and by comparison Mtr4, may be involved in both maintaining structural integrity and binding protein partners.[25]

Lastly, domain 4 (consisting of an 8 helix bundle) function is currently unknown. In Hel308 it is hypothesized that the helical bundle is involved in a "ratcheting" motion for transport of nucleic acid across the RecA-like domains by a central helix called the ratchet helix.[26] In Mtr4, the ratchet helix is positioned similarly to Hel308's ratchet helix bound to DNA. With all of the domains of Mtr4 interacting with nucleic acid, it is hard to pinpoint exactly how Mtr4 preferentially recognizes a short poly(A) sequence for its substrate. With the availability of the Mtr4 structures (apo-[27] and RNA-bound[28]) and the Hel308 structure, we are now in

position to perform a more detailed analysis in identifying potential residues of Mtr4 important for unwinding and sequence recognition (addressed further in Chapter 2).

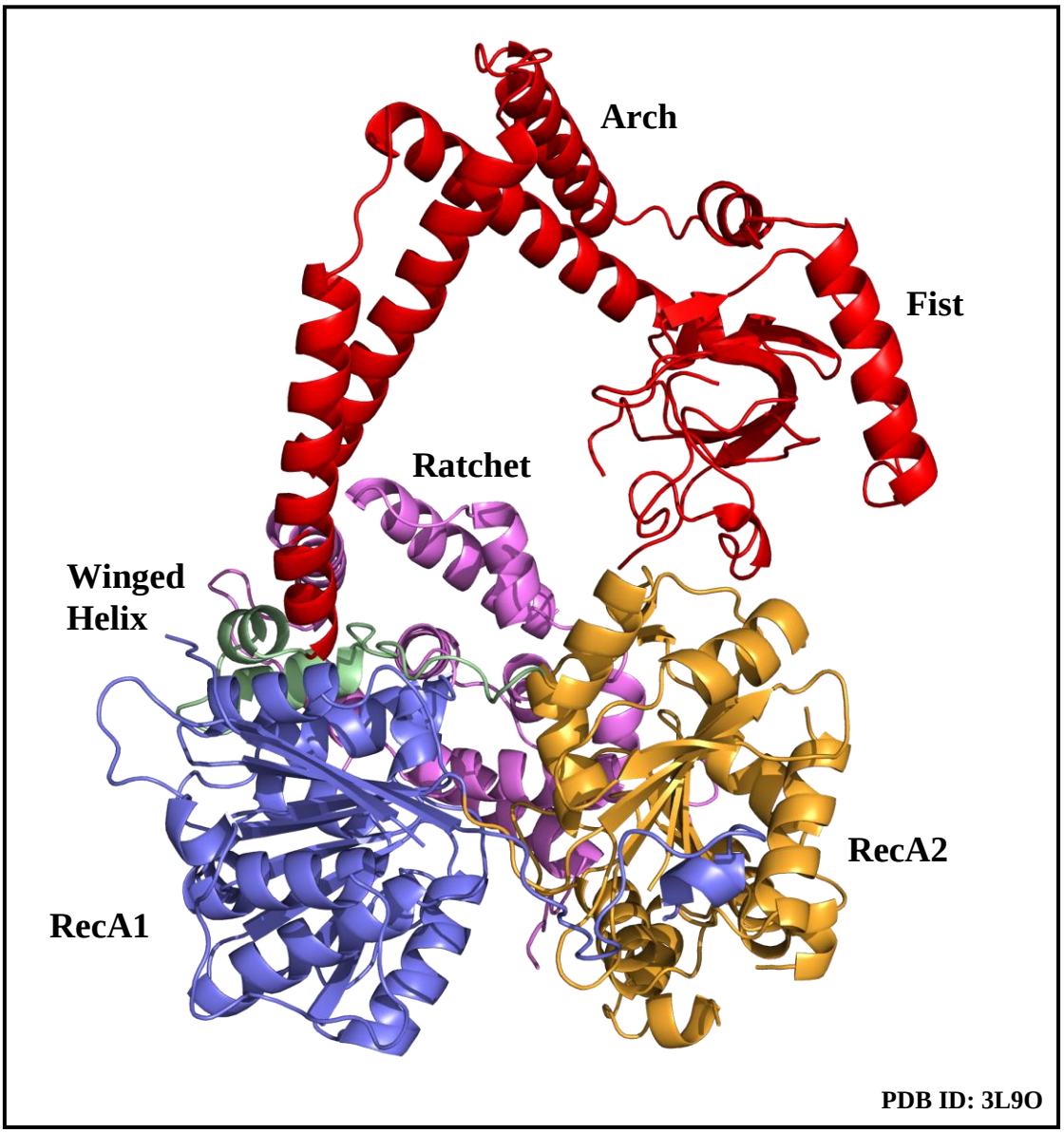

Figure 1-3. Structure of the RNA helicase Mtr4. The structure is colored and labeled by domain: RecA1 domain (slate blue), RecA2 domain (golden), Winged Helix domain (pale green), Arch domain (red), Ratchet domain (violet).

MTR4

Structural Insight Into Mtr4

In 2010, the first Mtr4 structure was published, providing new insight into the protein domains and their function. The structure of Mtr4 was observed to contain five distinct domains with a central channel having a diameter of ~ 12 Å.[27] As predicted domains 1 and 2 were the RecA-like domains consisting of a central β–sheet surrounded by α–helices.[27] These domains, however, consisted of exceptionally long β–sheets (10 strands). The winged helix (domain 3) was very similar to Hel308 with a root-mean-square deviation (RMSD) of 1.97 Å.[27] The function of the winged helix is still unknown, but a proposed function will be discussed further in the latter half of the introduction.

The most prominent feature of Mtr4 is the novel arch domain (or insertion domain 3a) which is specific to Mtr4 and Ski2.[27] The arch domain accounts for 25% of the entire protein, 265 residues inserted in the winged helix domain between the second and third helices.[27] The arch feature is characterized by an "arm" and "forearm" in which two anti-parallel helices[27] are joined through a sharp loop bent at ~ 120º. The "forearm" helix of the arch extends into the "fist" consisting of a central β–sheet surrounded by a globular α–β arrangement. The "fist" is structurally similar to the ribosomal protein L14e, indicating the potential for nucleic acid binding.[27] Domain 4 of Mtr4 consists of an eight-helix bundle and corresponds to a DSHCT domain found in DEAD box helicases.[27] This domain is structurally similar with the Hel308 structure, allowing for potential comparison with this well studied DNA helicase.

The Novel Arch Domain of Mtr4

Although no function has been attributed to the arch, it has been shown to bind structured RNAs. More specifically the fist portion of the arch domain alone is sufficient to

bind structured RNA such as $tRNA^{iMet}$ and rRNA.[28] When the arch is deleted there appears to be no effect on RNA unwinding *in vitro*.[27] However, the arch domain seems to be essential for proper maturation of the 5.8S rRNA from the 5.8S + 30, as determined by northern blot analysis.[27] An accumulation of the 5.8S + 30 rRNA is also seen when Rrp6 is knocked out. It was recently shown that when an mtr4-archless construct combined with an rrp6Δ construct was expressed, there was no increase in accumulation of the 5.8S + 30 rRNA suggesting that the arch domain of Mtr4 and Rrp6 share similar redundant functions.[29] However, an *in vivo* growth of the rrp6Δ and mtr4-archless mutant was no more severe of a slow growth phenotype than either of the individual mutants suggesting that the arch domain of Mtr4 is only required for certain functions of Rrp6 and may be necessary for other pathways.[29] Also, the arch domain is not necessary for TRAMP formation based on pull-down analysis.[19] However new evidence may provide a role for the arch in unwinding when associated with the ratchet helix, which will be discussed further in the results section in Chapter 2.

The Ratchet Helix

The Hel308 structure described the helical bundle domain (domain 4) to be a ratchet domain due to a central ratchet helix hypothesized to act as a directional transport of nucleic acids across the RecA-like domains.[26] *In vivo* analysis shows that a truncation of the ratchet domain in Mtr4 results in synthetic lethality, making this domain essential for Mtr4 viability.[19] The ratchet domain of Mtr4, consisting of an eight helix bundle, was not apparent by sequence to be similar to the Hel308 ratchet domain (11% sequence identity with 26% sequence similarity). However, when the Mtr4 structure was solved, the ratchet domain appeared to be structurally related to the Hel308 structure, with an RMSD of 2.7 Å.[27] Structural evidence of the ratchet helix interacting and presumably stabilizing base stacking interactions exists in the poly(A) RNA-bound Mtr4 structure.[28] This interaction between the ratchet helix and its RNA substrate in Mtr4 differs slightly from the interactions observed in

the Hel308 DNA-bound structure. It has been proposed that the variation in the ratchet helix between Hel308 and Mtr4 could be accounted for by their functional differences, such as substrate preferences.[22] Further investigation into this hypothesis is outlined in the results section in Chapter 2.

Substrate Specificity

Typically SF1 and SF2 helicases do not have sequence specificity for an RNA substrate *in vitro*.[30] However, Mtr4 has been shown to prefer a poly(A) substrate over a random sequence of nucleotides with a preferred substrate of 5 poly(A)'s on the 3' tail, the typical polyadenylated product of an RNA substrate targeted by TRAMP for the exosome.[31] The binding density mode, or length of nucleotides required for binding, was determined for Mtr4 to be approximately 5 nucleotides by Toth in 2010, using a Macromolecular Competition Titration Method. They discovered that this binding interface changed however when different nucleotides were bound. The binding density mode expanded to around 7 nucleotides long in the ADP-bound form and as large as 17 nucleotides long in the AMP-PNP-bound form (ATP analog) on a random substrate 20 nucleotides long. However, on a poly(A) substrate 20 nucleotides long, the binding density mode was relatively consistent at 5 nucleotides with or without ADP or AMP-PNP bound.[31] It was proposed that Mtr4 experiences conformational changes upon binding ATP that are substrate specific, and that the differences in the binding mode with the Mtr4-poly(A) compared to the Mtr4-random complex likely plays a role in Mtr4 recognition of sequence. Currently the mechanistic detail of sequence specificity is unknown for Mtr4, which is a topic that will be discussed further in the results/discussion section in Chapter 2.

TRAMP

Trf(4/5)-Air(1/2)-Mtr4 Polyadenylation (TRAMP4/5) complex

Other influences on Mtr4 substrate recognition could be attributed to binding partners of Mtr4. Several RNA helicases require cofactors to function properly.[21] Mtr4 interacts with various proteins in the cell, and some of these complexes appear to influence helicase function. Mtr4 is a member of the TRAMP complex, which is responsible for targeting and delivering RNA substrates to the nuclear exosome for degradation and maturation. TRAMP is composed of a poly(A) polymerase (Trf4/5), an RNA binding protein (Air1/2) and an RNA helicase (Mtr4). Substrates for polyadenylation by TRAMP include pre-rRNA, snRNA, snoRNA, tRNA, CUTs, and mRNA.[32] The degradation of such substrates relies on a polyadenylation event at the 3' end of the RNA by the non-canonical poly(A) polymerase Trf4/5. This 3' polyadenylation is quite different than canonical poly(A) polymerases that add a long stabilizing poly(A) tail to mRNA. Polyadenylation by TRAMP is a short poly(A) tail that destabilizes the RNA, targeting it to the exosome for processing or degradation.[33] Exactly how the Trf4/5 poly(A) addition is regulated to add a short extension of ~5 nucleotides is unclear, however, the RNA helicase component of TRAMP (Mtr4) has been shown to modulate this event.[34] Very few *in vitro* studies of the TRAMP complex have been done to characterize the function of these three components, each having their own distinct function. The TRAMP complex is quite unstable, only withstanding up to 200 mM NaCl, at which point Mtr4 dissociates from Trf/Air proteins.[35] The complex is incredibly delicate to purify in its active form, and therefore difficult to characterize biochemically as well as crystallize for structural determination.

TRAMP modulation

Several *in vivo* studies have identified target substrates for TRAMP through accumulation of various RNAs when components of the TRAMP complex have been knocked down. When TRAMP is functioning improperly, an accumulation of a poly(A) tail on an immature RNA substrate of TRAMP is observed, which is how most substrates of TRAMP have been identified (also by immunoprecipitation assays). The first *in vitro* characterization of poly(A) modulation was published in 2011 by the Jankowsky lab. They showed that the poly(A) tail addition would reach a maximum rate that correlated to a 4-5 poly(A) extension, and gradually slow down for any additional adenylation.[36] TRAMP was then tested on duplexed and single-stranded RNAs as well to determine if unwinding had an effect on adenylation. However, the single stranded substrate was polyadenylated at roughly the same rate and trend as the duplexed RNA.[36] Surprisingly, when polyadenylation was monitored with just Trf4-Air2 (no Mtr4), the rate of poly(A) addition gradually increased over time with no optimal tail length.[36] Interestingly enough, an E947A mutation of Mtr4 resulted in a loss of modulation of Trf4 polyadenylation.[36] Thus, Mtr4 is important in modulating the length of poly(A) tail addition to around 4-5 nucleotides; however this modulation by Mtr4 is not dependent on its helicase function.

Monitoring Mtr4's function in the context of TRAMP (with inactive Trf4) revealed some exciting new discoveries about Mtr4's unwinding activity. Mtr4 helicase activity was shown to enhance nine-fold in the context of TRAMP on a short duplex (16 bp) RNA with a 25 nt overhang on the 3' end.[37] These same trends were also observed on a 36 bp RNA duplex with a 25 nt overhang.[37] Since most DEAD-box family helicases unwind substrates with approximately one and a half turns (~16 bp), the fact that TRAMP and Mtr4 alone unwound a 36 bp duplexed region is quite fascinating. DNA and RNA duplexes, as well as hybrids, were also tested on Mtr4 and TRAMP to see what type of substrates are required for unwinding based on previous characteristics of DEAD-box helicases. Neither TRAMP nor

Mtr4 alone unwound a DNA duplex (16 bp) with a 25 DNA nt overhang on the 3' end.[37] The only hybrid variation that TRAMP and Mtr4 unwound (with the same enhancement in rate by TRAMP as seen previously) was a DNA top strand (16 nt) duplexed to an RNA bottom strand, with a 25 nt overhang on the 3' end.[37]

To find the preferred length of 3' overhang, a RNA duplex (16 bp) with a one nucleotide overhang was attached to biotin tagged beads. A simultaneous polyadenylation and unwinding reaction was then performed with wild-type TRAMP.[37] When substrates were analyzed, the polyadenylated strand of RNA was released and found to contain at least four adenylates.[37] This result suggested that a minimum of 5 nt are required on the 3' end for Mtr4 to unwind. Helicase assays confirmed this result showing that no unwinding occurs with a 4 nt overhang, and optimal unwinding occurs with a 6 nt overhang in TRAMP

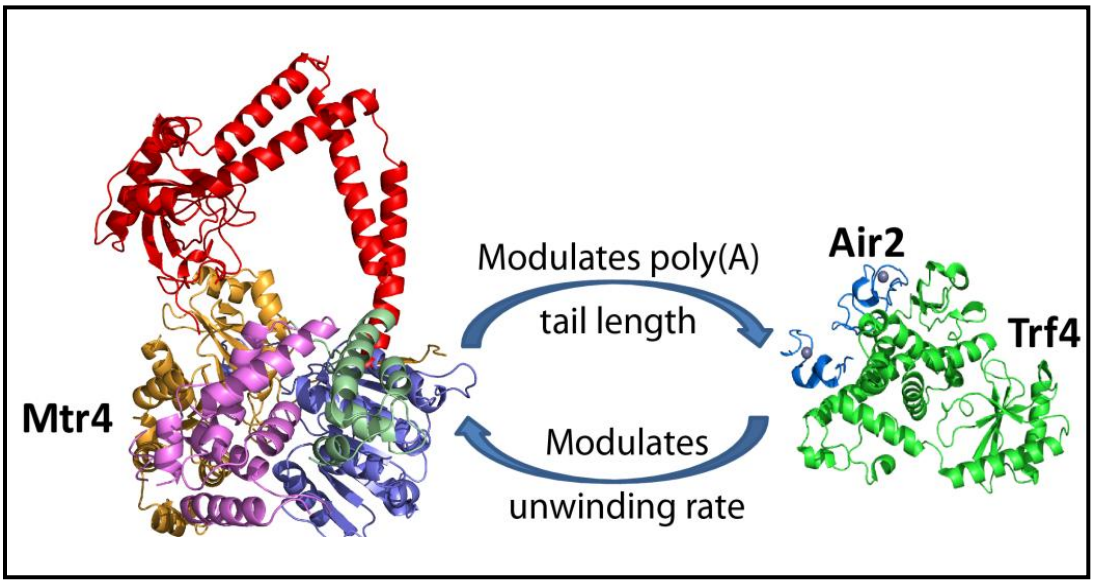

Figure 1-4. Outline of the modulation events within the TRAMP complex.

independent of the actual polyadenylation process.[37] The mechanistic detail of unwinding by Mtr4 alone and in the context of TRAMP is still poorly understood (Figure 1-4), however

studies such as the one previously mentioned are providing insight into the capabilities of this complex.

CONCLUSION

All aspects of eukaryotic RNA metabolism involve RNA helicases. Understanding the mechanism by which Mtr4 recognizes substrates and unwinds them is important to understanding and maintaining RNA processing pathways. Keeping RNA levels regulated and functioning properly, with the aid of the exosome, is crucial in order to maintain healthy cells. As mentioned earlier, if RNA surveillance is not monitored properly diseases such as polymyositis/scleroderma-overlap syndrome will occur. Therefore, the need to understand how these proteins function at the mechanistic level is important to help maintain proper RNA surveillance. Little is known as to how Mtr4 functions in recognizing substrates and unwinding them. Two structures of Mtr4 exist, an apo- and a 5 nt poly(A) RNA-bound; however, insight into RNA sequence recognition by Mtr4 is still unclear. The RNA bound structure of Mtr4 displayed two different binding interfaces with substrate within the same crystal. Through the analysis of the structure of Mtr4, key residues along the ratchet helix were identified as mutagenesis targets for studying the binding interface with RNA substrates. The significance of these residues to Mtr4 function has yet to be addressed, neither through the use of activity assays nor crystallographic studies. Therefore, biochemical studies probing RNA substrates with varying mutations of Mtr4 will be useful in concurrence with a native RNA-bound structure of Mtr4 to elaborate on the mechanistic detail of substrate recognition.

CHAPTER 2

THE MTR4 RATCHET HELIX FUNCTIONS IN CONCERT WITH THE ARCH DOMAIN TO REGULATE HELICASE ACTIVITY[1]

ABSTRACT

Mtr4 is a conserved superfamily-2 RNA helicase that activates exosome mediated 3'-5' turnover in nuclear RNA surveillance and processing pathways. As a member of the Trf(4/5)-Air(1/2)-Mtr4 polyadenylation (TRAMP4/5) complex, Mtr4 is understood to unwind polyadenylated RNA substrates and present them to the exosome for degradation. Prominent features of the Mtr4 structure include a four domain ring like helicase core and a large arch domain that spans one side of the core. Within the helicase core, a "ratchet helix" is positioned to interact with the bases of unwound RNA substrates. However, the contribution of these interactions to Mtr4 activity is poorly understood. Here we show that conservation along the ratchet helix is particularly extensive for Mtr4 as compared to related helicases. Mutation of residues along this helix alter RNA unwinding rates in both an Mtr4 and TRAMP context, and result in slow growth phenotypes *in vivo*. We further observe that R1030 on the ratchet helix influences Mtr4 affinity for polyadenylated substrates. Previous work indicated that deletion of the arch domain had minimal effect on Mtr4 unwinding activity. Surprisingly, we now show that the combination of archless and ratchet helix mutations completely abolishes helicase activity and produces a lethal *in vivo* phenotype. These studies demonstrate that the ratchet helix modulates helicase activity, and suggests that the arch domain plays a previously unrecognized role in unwinding substrates.

---

1. Coauthored by Lacy Taylor, Ryan N Jackson, A. Alejandra Klauer, Megi Rexhepaj, Lindsey K Lott, Ambro van Hoof and Sean J Johnson; Manuscript in progress.

INTRODUCTION

To maintain correct gene expression in the cell, the integrity of RNA must be tightly regulated through RNA processing, turnover and surveillance pathways.[38-40] Several disease states are linked to defects in RNA quality control mechanisms, including neurodegenerative diseases, congenital diseases and cancer.[41-45] The eukaryotic exosome, which contains both endonuclease and 3'-5' exonuclease activities, plays a critical role in a wide variety of RNA processing and degradation pathways.[9,46-48] Regulation of this activity involves multiple protein cofactors including the nuclear Trf4-Air2-Mtr4 polyadenylation (TRAMP4) complex.[49-51] TRAMP facilitates the 3'-end processing of rRNAs, snoRNAs, and snRNAs as well as the degradation of cryptic unstable transcripts (CUTs), aberrant RNAs, antisense RNAs, intronic RNAs, several mRNAs and incorrectly processed RNAs.[9,52-55] TRAMP is also involved in transcriptional regulation, chromatin maintenance and DNA repair.[53,56-58]

TRAMP is composed of a poly(A) polymerase (Trf4 or Trf5), a zinc knuckle RNA binding protein (Air2 or Air1) and a Ski2-like RNA helicase (Mtr4) that are conserved throughout eukaryotes.[49-51] Reminiscent of RNA degradation pathways observed in prokaryotes and organelles,[59,60] TRAMP promotes 3'-5' exosomal degradation by adding a short 4-5 nt poly(A) tail to the 3' end of RNA.[33,34] Depletion or mutation of Mtr4 causes a buildup of polyadenylated TRAMP substrates, demonstrating that Mtr4 is the fundamental link between TRAMP and exosome degradation.[61-62] The helicase activity of Mtr4 is proposed to resolve secondary structures and remove proteins associated with the RNA, thus facilitating delivery of single stranded RNA to the exosome.[52,54-59]

Mtr4 binds poly(A) RNA with higher affinity and with a mechanism distinct from that employed to bind non(A) sequences.[20,31] Mtr4-substrate interactions are dynamic and are dependent on substrate length and the presence of bound nucleotide. The ability of Mtr4 to distinguish poly(A) from non(A) substrates in the absence of nucleotide is enhanced 10-fold as the length of the RNA substrate is reduced from 20 to 5 nucleotides, the minimal Mtr4

binding site.[31] Notably, two *in vitro* studies by Jia et al demonstrate that not only does Mtr4 show an unwinding preference for substrates with poly(A) tail overhangs one binding site long,[37] the polyadenylation activity of TRAMP is restricted by Mtr4 to maintain this optimal tail length in targeted RNAs.[36] Furthermore, a UV cross-linking study in yeast recently determined that Trf4 substrates contain an average poly(A) tail length of 5 nucleotides, supporting the conclusion that poly(A) tail length is regulated *in vivo*.[33] Mtr4 contains a fine tuned mechanism that senses the number and identity of 3' end poly(A) tracts, potentially through distinct interactions with the TRAMP complex that modulates both polymerase and unwinding activities. However, it is unclear how Mtr4 senses the length and identity of the sequence, and how this sensing is coupled to unwinding.

Recent crystal structures of Mtr4, including apo- and RNA-bound forms, and several related Ski2-like and DEAH/RHA-box helicase structures provide insight into the general features employed by these helicase families to bind and translocate along nucleic acid substrates.[27,28,63-69] Although each helicase exhibits unique features and accessory domains, they all contain a common core structure composed of two RecA domains (Mtr4 domains 1 and 2), a winged helix domain (domain 3), and a 7-8 helix bundle domain[22] (domain 4). In the case of the Ski2-like RNA helicase Brr2, two helicase cores are connected in tandem, with only the first core being active *in vitro* and *in* vivo.[70,71] The RecA domains contain conserved sequence motifs that bind nucleic acid, and bind and hydrolyze ATP.[72] The Hel308 DNA helicase structure bound to duplex DNA shows a β-hairpin within the second RecA domain facilitates strand splitting as the nucleic acid enters the helicase core.[63] The 3' single stranded nucleic acid then traverses the RecA domains and interacts with domain 4 before exiting at the base of the helicase core. Multiple interactions are observed with domain 4, particularly along the "ratchet helix" where nucleotides stack with W599 and R592 in a manner that is thought to facilitate DNA translocation in Hel308.[63] Not surprisingly, deletion of domain 4 abolishes helicase activity in Hel308,[63] and the analogous mutation in

Mtr4 is unviable *in vivo*.[19] In a related Ski2-like helicases Brr2, a point mutation in domain 4 (R1107A, similar to W599 in Hel308) conferred a slow growth phenotype and loss of *in vitro* activity.[70,73] Although domain 4 appears to play an important role in helicase activity, a mechanistic description of domain 4 function is lacking, particularly for Ski2-like RNA helicases.

In an effort to better characterize the Mtr4 RNA binding path, we have investigated amino acid residues along the ratchet helix of domain 4. Sequence and structural analysis reveals discrete conservation patterns in Mtr4, Ski2-like and DEAH/RHA-box helicases. Mutagenesis studies demonstrate that R1030 and E1033 play important, but distinct roles in sequence recognition and helicase activity. *In vivo* analysis further underscores the importance of ratchet helix residues for cellular function. Additionally, we identified arch involvement in unwinding activity when combined with either ratchet helix point mutant. These data suggest that residues along the ratchet helix provide a mechanism for regulating helicase activity and in concert with the arch domain are essential for unwinding activity and cell viability.

MATERIALS AND METHODS

Structural Analysis and Conservation Scoring of Ski2-like and DEAH/RHA Box Helicases

The helix-bundle domain (domain 4) of archaeal Hel308 (pdb 2P6R)[33] was used as bait in a DALI search[74] to find structures containing a helix-bundle domain with an associated ratchet helix. Conservation of eukaryotic helicases was determined by multiple sequence alignment of model organisms in CLUSTALW[75] and conservation scoring with the ConSurf server.[76] For the archaeal Ski2-like DNA helicase Hel308, 98 archaeal sequences including the sequences of existing Hel308 structures were retrieved and scored using the ConSurf server. ConSurf scores of 10, 9, and 8 were considered conserved.

Mutagenesis, Protein Expression and Protein Purification

Point mutants of Mtr4 were made using a modified version of the QuikChange (Agilent) site directed mutagenesis procedure. The expression and purification of Mtr4 and mutant Mtr4 proteins was carried out as performed previously.[27] No differences in expression were observed between the mutants and wild-type protein. However, the R1030A Mtr4 variant exhibited poor solubility, yielding low amounts of protein. Protein concentration was determined using a NanoDrop spectrophotometer (Thermo Fisher) and calculated extinction coefficients. Expression and purification of TRAMP complexes was performed essentially as by Jia et al.[37] Specifically, Cell lysis was performed by lysozyme treatment and sonication of frozen cell pellets. Cobalt affinity, FLAG affinity, and NAP-25 gel filtration was used to purify TRAMP complexes at 4ºC. Purification buffers consisted of 50 mM sodium phosphate buffer (pH 7.0), 10% glycerol, 10 μM $ZnCl_2$. Salt concentration varied from 250 mM NaCl at lysis, to 200 mM NaCl final concentration.

RNA Substrate Design and Purification

The RNA substrates were designed to mimic unwinding substrates used in the recent study by Jia et al.[37] These 22 nucleotide ssRNAs (each with a unique 3' end) were incubated independently with a complementary 16 nucleotide ssRNA at 95°C for 10 minutes after which samples were slowly annealed to room temperature.

The 16 nucleotide top strand was radiolabeled with γ-^{32}P ATP and T4 polynucleotide kinase and quenched by heating to 95°C before annealing. The RNA substrates were purified by native PAGE, gel extraction and ethanol precipitation. All RNAs used in this study were purchased from Integrated DNA Technologies (IDT). The substrate sequences are as follows with duplex regions underlined:

R16 (top strand of all three substrates) = 5'<u>AGCACCGUAAAGACGC</u>3',
R22A (poly(A) overhang) = 5'<u>GCGUCUUUACGGUGCU</u>UAAAAA3',
R22R (non(A) overhang) = 5'<u>GCGUCUUUACGGUGCU</u>UGCCUG3'.

Unwinding Assay

Pre-steady state unwinding assays were performed essentially as described by Jia et al.[37] A radiolabeled 16 nucleotide strand was displaced over time when incubated with Mtr4 and saturating levels of ATP. Reactions were carried out at 30°C in a controlled water bath. The buffer used was 40 mM MOPS pH 6.5, 100 mM NaCl, 0.5 mM $MgCl_2$, 5% glycerol, 0.01% NP-40 substitute, 2 mM DTT, and 1 U/µl of Ribolock (Thermo Fisher). Reactions were allowed to incubate for 5 minutes with ~0.2 nM RNA (final concentration) and the indicated concentration of Mtr4 or Mtr4 mutant protein in Figure 2-4. Reactions were initiated by the addition of equimolar ATP and $MgCl_2$ at a final concentration of 1.6 mM. At specified time points, aliquots of the reaction were removed and quenched at a 1:1 ratio with buffer containing 1% SDS, 5 mM EDTA, 20% glycerol, 0.1% bromophenol blue and 0.1% xylene cyanol. Aliquots were run on a native 15% TBE polyacrylamide gel at 100 V for 115 minutes. Radioactivity was visualized as performed previously.[27] Gels were wrapped in cellophane and exposed to x-ray film or phosphor screen. Film was developed and then quantified using multi-gauge software; phosphor screen was developed by a Storm PhosphorImager (Amersham Biosciences) and quantified using ImageQuant software. Calculations of the observed rate constants (k_{unw}), and amplitudes (A) were performed using integrated first-order rate law. Curve fits were made to data collected in triplicate, as employed previously (Fraction unwound = $A(1-\exp(-k_{unw} \cdot t))$.[27,37,77] The k_{unw}^{max} and $K_{1/2}$ values were calculated using best fit curves as done by Jia et al,[37] with the equation, $k_{unw} = k_{unw}^{max}, _E [E]/[E] + K_{1/2}, _E$, where [E] is enzyme concentration, $K_{1/2}$ is functional affinity and $k_{unw}^{max}, _E$ is the unwinding rate constant at enzyme saturation.

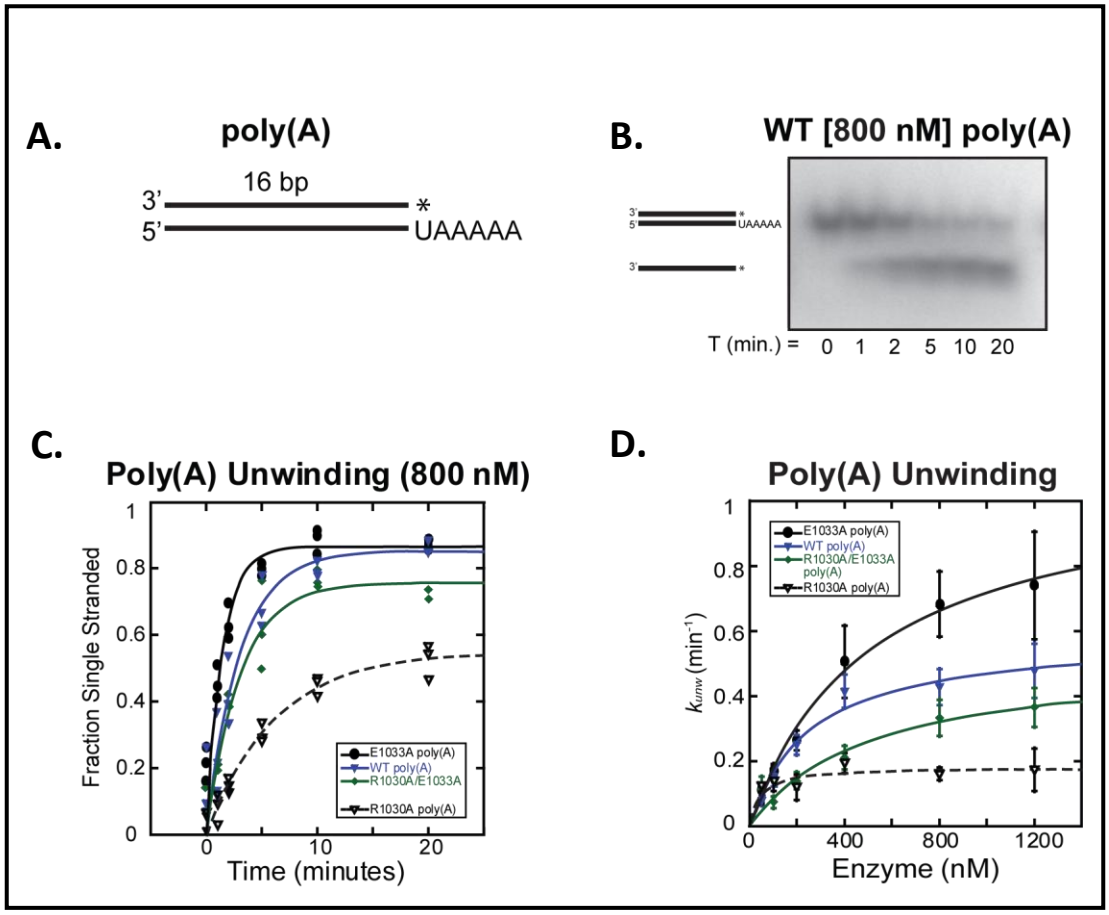

Figure 2-1. Unwinding assays of ratchet helix point mutants. (A) The RNA substrate used in this study was the 16 bp duplex with a 3' end poly(A) overhang. (B) Native PAGE experiment demonstrating the unwinding of Mtr4 wild type with a 5'-^{32}P radiolabeled poly(A) substrate. (C) Representative time course of fraction unwound values of wild type (WT), R1030A, E1033A, and R1030A/E1033A Mtr4 enzymes with poly(A) RNA . The integrated first-order rate law was utilized to generate a best fit curve to the data and the unwinding rate constant (k_{unw}). (D) Unwinding rate constants of poly(A) RNA plotted against the concentration of Mtr4 enzymes. The curves represent the best fit to the equation $k_{unw} = k_{unw}^{max}, {}_{E}[E]/([E] + K_{1/2}, {}_{E})$; k_{unw}^{max} is the maximum unwinding rate, [E] is the enzyme concentration, and $K_{1/2}$ is the functional affinity.

Yeast plasmids

The plasmids for expression of Mtr4-wild-type or Mtr4-ratchet helix mutants contained the same upstream promoter and downstream sequence as used previously.[27] The same wild type MTR4 expression plasmids pAv673 (a URA3 CEN plasmid[78]), and pAv675

(a LEU2 CEN plasmid[78]) were used as previously described.[27] Plasmids expressing ratchet helix mutants are simply point mutants of pAv675.

Yeast methods

An MTR4 deletion strain of *Saccharomyces cerevisiae* complemented with a MTR4-wild-type copy plasmid containing a URA3 selectable marker was transformed with MTR4-wild-type or MTR4-ratchet helix mutant plasmids. Resulting transformants were grown in Synthetic Complete-LEU (SC-LEU) liquid media overnight at 20°C, 30°C, and 37°C to test if the mutation caused growth defects. Liquid cultures were serial diluted five-fold and spotted onto control plates (SC-LEU) or 5-fluoro-orotic acid (5-FOA; to counter against the MTR4-wild-type plasmid containing URA3 selectable marker).

RESULTS

Structural Analysis of the Mtr4 RNA Binding Path Reveals Distinct Modes of Substrate Binding

In the RNA-bound structure of Mtr4, two molecules are observed in the asymmetric unit.[28] In both molecules, a 5 nt poly(A) RNA substrate interacts with the canonical helicase motifs of the RecA domains 1 and 2 through multiple phosphate backbone interactions, similar to that observed in Hel308[63] (Figure 2-2). Domain 4 is positioned on the opposite side of the RNA and interacts directly with the nucleotide bases. The primary base interactions in Mtr4 are with E947, located on a loop above the ratchet helix, R1026, R1030, and E1033, which occupy one face of the ratchet helix. Notably, each of these base interactions appear to be mediated through hydrogen bonds, whereas interactions in Hel308 generally involve base stacking, Figure 2-2. The direct protein-nucleotide base interactions observed in the Mtr4 crystal structure suggest that the function of the ratchet helix may not be

restricted to RNA translocation (by analogy to Hel308), but may also involve RNA sequence recognition.

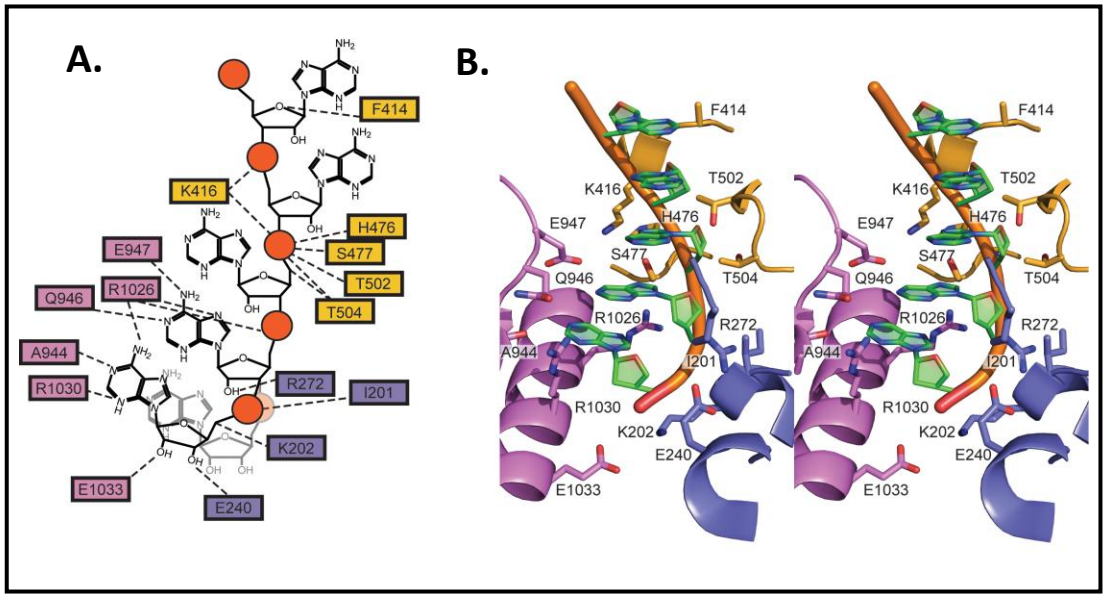

Figure 2-2. Cartoon schematic and structural depiction of the RNA-protein interface of Mtr4 with a 5 nt poly(A) substrate. (A) Diagram of molecule B of Mtr4 highlighting the RNA-protein interface, with key interactions shown in dashed lines. (B) Stereo view of the structure of molecule B of Mtr4 showing the correct spatial arrangement of the interacting residues with the RNA substrate.

Ratchet Helix Residues are Conserved in Ski2-like/DExH-box Helicases

We next examined the conservation of the residues along the ratchet helix for the Ski2-like Mtr4, Ski2, Brr2, and Hel308 helicases and the DEAH/RHA-box Prp22 and Prp43 helicases.[68,69-71] CLUSTALW was used to align a diverse set of eukaryotic sequences for each helicase[75] (archaeal sequences were used for Hel308). Conservation scores were calculated using the ConSurf server.[76] Extensive conservation is observed along the entire ratchet helix for the Ski2-like RNA helicases (Mtr4, Ski2 and Brr2) (Figure 2-3 C). Less conservation is observed for Hel308 and the DEAH/RHA-box RNA helicases Prp22 and Prp43 (Figure 2-3 C and D). In the case of Hel308, position W599 is the only strictly

conserved ratchet helix residue observed to interact with nucleic acid. The conserved residues observed at the N-termini of each helix are involved in interactions with domain 2 and generally do not interact directly with nucleic acid. However, R1026 of molecule B of Mtr4 is modeled to interact with base 5 of the RNA strand.

Although no residue along the ratchet helix is universally conserved throughout helicases, conservation patterns are clearly evident. The most striking feature is that the fourth turn of the ratchet helix (counting from the N-terminus) is strictly conserved in a helicase-specific manner (Figure 2-3 D). Mtr4 and Ski2 always have a glutamate at the same position on the fourth turn (E1033 in Mtr4; E1247 in Ski2), Brr2 has an arginine (R1107), Prp22 and Prp43 have a glutamine (Q1081 in Prp22; Q622 in Prp43), and Hel308 has a tryptophan (W599). Among the Ski2-like RNA helicases, we note similar conservation

Figure 2-3. Conserved ratchet helix residues interact with nucleic acid. (A) The RNA-bound Mtr4 structure (PDB 2XGJ) molecule A is colored by domains. (Inset) Helix-bundle domain (domain 4) residues that interact with poly(A) RNA are shown as sticks, molecule B aligned residues and RNA bases are colored cyan and light blue respectively. Nucleotides are labeled 1-5. (B) The DNA-bound Hel308 structure (PDB 2P6R) is colored by domains. Inset image highlights the pi stacking interactions of ratchet helix residuesW599 and R592 shown as sticks with bases of ssDNA. Nucleotides downstream of the strand splitting β-hairpin are labeled +1 through +5. (C) Alignment and conservation scores (calculated using Consurf) of eukaryotic Mtr4 and archaeal Hel308 ratchet helix sequences. Conservation is colored strictly conserved as orange, to variable as white. Extensive conservation at helical turn 4 is highlighted with an arrow. Alignment of Mtr4 includes 10 model eukaryotic species (S.cer, *Saccharomyces cerevisiae*; S.pom, *Schizosaccharomyces pombe*; N.cra, *Neurospora crassa*; H.sap, *Homo sapiens*; M.mus, *Mus musculus*; D.rer, *Danio rerio*; D.mel, *Drosophila melanogaster*; C.ele, *Caenorhabditis elegans*; M.bre, *Monosiga brevicollis*; A.tha, *Arabidopsis thaliana*). Alignment of Hel308 includes the sequences of crystal structure homologs and 7 other archeal sequences (A.ful, *Archaeoglobus fulgidus*; S.sul, *Sulfolobus solfataricus*; P.fur, *Pyrococcus furiosus*; P.hor, Pyrococcushorikoshi; A.ven, *Archaeoglobus fulgidus*; F. pla, *Ferroglobus placidus*; M.the, *Methanosaeta thermophila* S.hel, Staphylothermus hellenicus; T.vol, *Thermoplasma volcanium* P.aci, *Candidatus Parvarchaeum acidophilus*; M.kan, *Methanopyrus kandleri*) (D) Conservation of Ski2-like and DEAH/RHA-box helicases are mapped onto a ratchet helix cartoon depicting the observed sequences. The sequence placement of the S1 ratchet of Brr2 was performed using a previously determined alignment.[71,79] Extensive conservation at helical turn 4 is highlighted with an arrow.

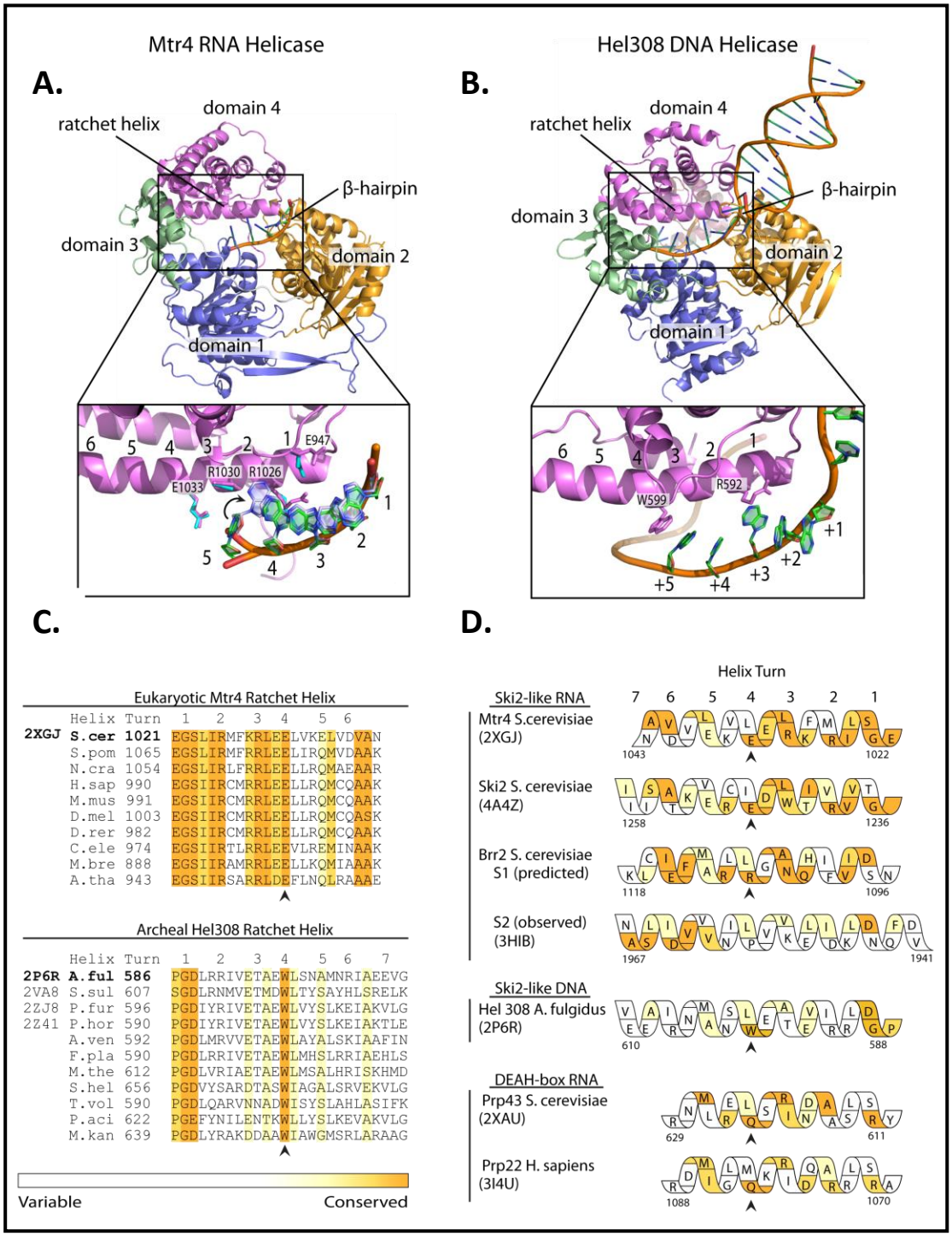

patterns at the second and third turns of the ratchet helix. In the case of Mtr4, both positions are always arginines (R1026 and R1030).

R1030 and E1033 Play Distinct Roles in Unwinding

The interaction of R1030 and E1033 with RNA observed in the Mtr4 structures combined with the strong conservation at each of these positions in Ski2-like RNA helicases suggested that these residues might be important for Mtr4 activity. To assess the role of these residues in Mtr4 function, we mutated each position in *S. cerevisiae* Mtr4 to alanine (R1030A, E1033A). E1033 was also mutated to tryptophan (E1033W) to mimic the sequence observed in Hel308. Pre-steady state unwinding assays and calculations were performed using a helicase assay developed previously to characterize the unwinding activity of Mtr4 and other helicases.[37,80] The assay detects the displacement of a ^{32}P labeled top strand from complementary bottom strand with a 3' single-stranded extension of 6 nt (Figure 2-1).

Using a 3' polyadenylated substrate (poly(A)), we observed a smaller unwinding constant (k_{unw}) for the R1030A Mtr4 mutant at 800 nM protein than that observed for wild-type enzyme (Figure 2-1 C). In contrast, the E1033A protein demonstrated a higher k_{unw} at 800 nM than wild-type Mtr4 (Figure 2-1 C). Interestingly, when mutated to a tryptophan, this construct showed significantly less unwinding activity than wild-type Mtr4 on a poly(A) substrate (Figure 2-1). Unwinding rate constants (k_{unw}) at several concentrations were determined for the ratchet helix mutants to obtain the strand-separation rate constants at enzyme saturation (k_{unw}^{max}) (Figure 2-4 and Table 2-1). Compared to wild-type, the R1030A and E1033W mutants displayed a lower k_{unw}^{max} and the E1033A mutant displayed higher k_{unw}^{max}, demonstrating that residue identity at specific ratchet helix positions directly influences the strand-separation rate constant.

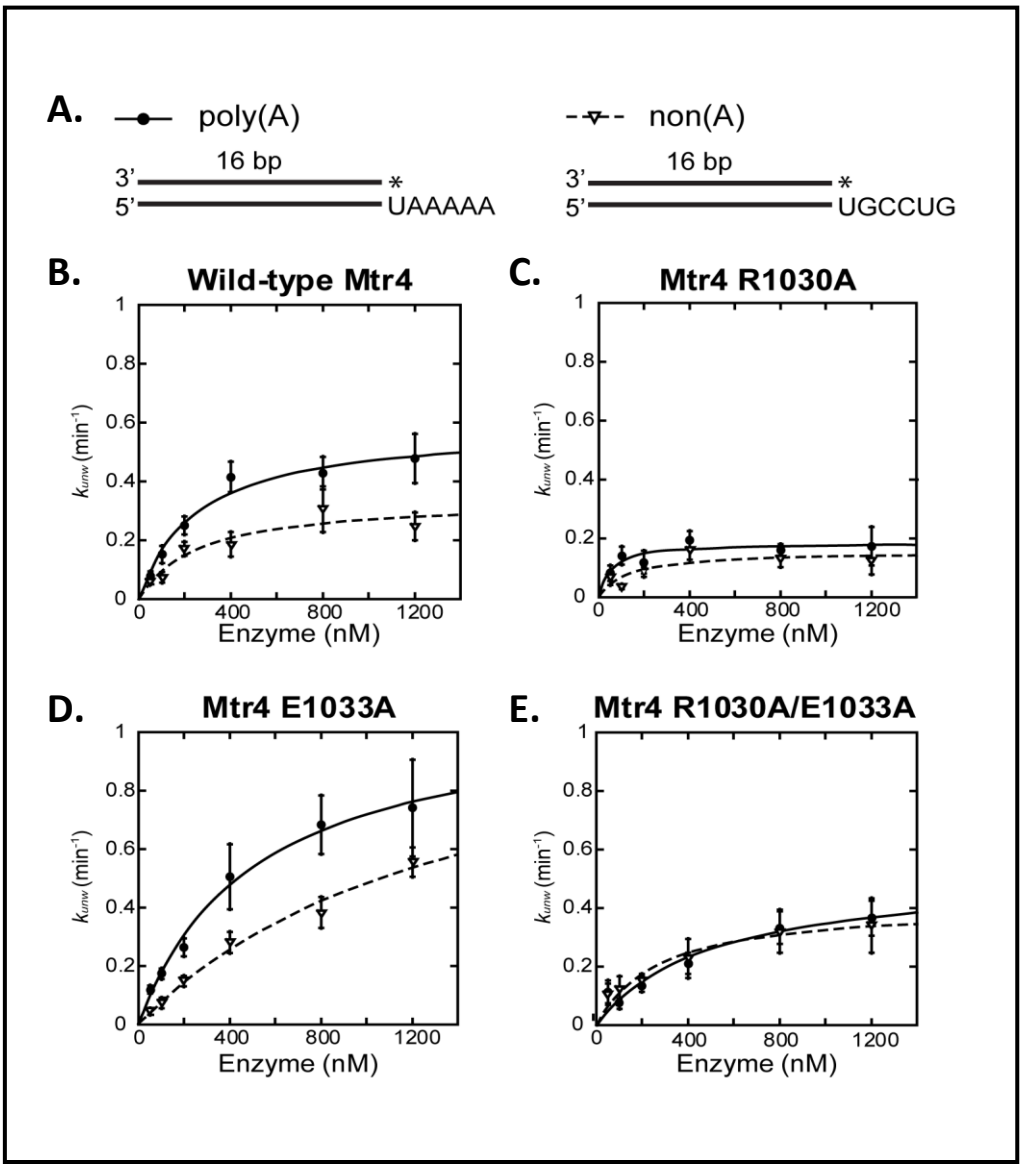

Figure 2-4. Unwinding assays of ratchet helix point mutants. (A) The RNA substrates used in this study, poly(A) and non(A), have identical 16 bp duplex regions (see methods for full sequence details) with variable 3'end overhangs. Radiolabel is indicated by an asterisk. (B) Plotted unwinding rate (k_{unw}) constants at different concentrations of wild-type (WT) Mtr4 enzyme with poly(A) and non(A) RNA substrates. Shown are best fit curves to the data using the integrated first-order rate law $k_{unw} = k_{unw}^{max}{}_{,E}\,[E]/([E] + K_{1/2,\,E})$. (C) Plotted unwinding rate constants and curve fits for the R1030A mutant enzyme with poly(A) and non(A) RNA. (D) Plotted unwinding rate constants and curve fits for the E1033A mutant enzyme with poly(A) and non(A) RNA. (E) Plotted unwinding rate constants and curve fits for the R1030A/E1033A mutant enzyme with poly(A) and non(A) RNA.

R1030 is Involved In Sequence Recognition

To study the effects of different RNA sequences on the unwinding activity of Mtr4 ratchet helix mutants, we determined unwinding rate constants for a non-polyadenylated substrate (non(A)) used recently to characterize Mtr4 sequence preference)[27] (Figure 2-4, and Table 2-1). Wild-type and E1033A Mtr4 enzymes showed an unwinding preference for the poly(A) substrate over the non(A) substrate at all enzyme concentrations tested. In contrast, Mtr4 enzymes containing the R1030A mutation displayed roughly identical k_{unw} values at each concentration. To further characterize the impact of the E1033 and R1030 mutation, we tested the double alanine mutant R1030A/E1033A for unwinding activity. The R1030A/E1033A mutant unwound the substrate faster than R1030A alone, however it did not regain the ability to differentiate between a poly(A) and a non(A) substrate. Our data clearly demonstrate a preference for the poly(A) substrate in wild-type and E1033A enzymes that is no longer observed in enzymes containing the R1030A mutation. This is the first identification of a residue of Mtr4 involved in recognition of substrates with a poly(A) tail.

R1030 and E1033 Are Important for Mtr4 Function in Vivo

After determining that the R1030 and E1033 residues play a significant role in Mtr4 helicase activity *in vitro*, we wanted to explore how mutations at ratchet helix positions affect Mtr4 function *in vivo*. Mutants, *mtr4*-R1030A, E1033A, E1033W and the double mutant *mtr4*-R1030A/E1033A were constructed, serially diluted, and tested for viability at 20ºC, 30ºC, and 37ºC. Complementation with plasmid containing wild-type MTR4 was used as a positive control, whereas *mtr4-archless* and *mtr4*-D262A/E263A mutants were used to demonstrate a slow growth phenotype and an active site knockout respectively. The ratchet helix mutations confer a slow growth phenotype at all temperatures tested, demonstrating that these residues are important for Mtr4 function *in vivo* (Figure 2-5 A). At 30ºC, the growth

Table 2-1. Kinetic constants of Mtr4 constructs with the poly(A) and non(A) overhang substrate. For the poly(A) and non(A) substrates, $K_{½}$ and k_{unw}^{max} values are given for wild-type Mtr4, R1030A, E1033A, the double mutant R1030A/E1033A, the double mutant R1030A-Archless, and the double mutant E1033A-Archless.

	poly(A)		non(A)	
Enzyme	$K_{½}$ (nM)	k_{unw}^{max} (min^{-1})	$K_{½}$ (nM)	k_{unw}^{max} (min^{-1})
WT	251.86 ± 59.95	0.59 ± 0.05	254.65 ± 116.39	0.34 ± 0.05
R1030A	51.29 ± 26.36	0.18 ± 0.02	128.9 ± 92.19	0.16 ± 0.03
E1033A	504.09 ± 92.89	1.08 ± 0.09	1415.2 ± 467.6	1.17 ± 0.24
E1033W	483.81 ± 359.66	0.22 ± 0.07	Not tested	Not tested
R1030A/E1033A	498.11 ± 215.81	0.52 ± 0.10	268.72 ± 80.87	0.41 ± 0.04
R1030A-Archless	no activity detected			
E1033A-Archless	no activity detected			

[a]Methodologies and equations used to derive kinetic constants are found in the materials and methods section.

defect appears to be most pronounced for the R1030A mutation. Surprisingly, the greater growth defect of *mtr4*-R1030A is suppressed by the E1033A mutation as seen in the *mtr4*-R1030A/E1033A double mutant. At 37ºC growth defects were even more pronounced and the pattern appeared to change with the E1033W mutant and the R1030A/E1033A double mutant mimicking the R1030A mutant. Regardless of temperature, however, the double mutation did not compound the growth phenotype observed at single sites, suggesting that defects caused by each ratchet helix mutation reside in the same mechanistic pathway.

Notably, while each of the ratchet helix mutants confered a slow-growth phenotype, none of the mutants were as detrimental as the arch deletion (archless) on cell viability. The arch of Mtr4 is known to bind RNA *in vitro*, however unwinding activity in an arch knockout does not alter unwinding rates.[27] To further probe the effect of these mutations, we paired the ratchet helix mutants with an archless mutant of Mtr4. Mutants, *mtr4*-R1030A-*archless* and

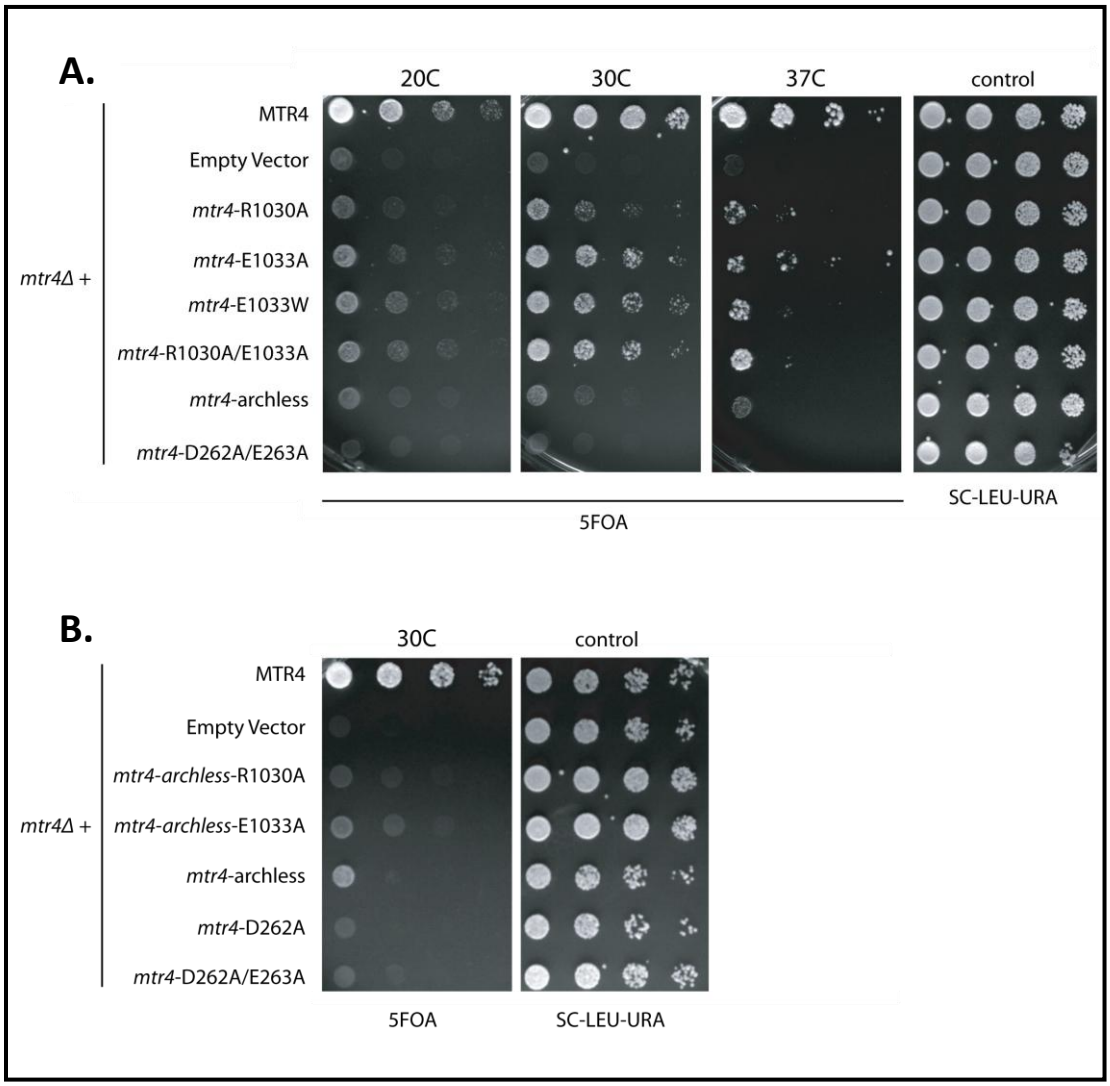

Figure 2-5. Growth complementation of an Mtr4 knockout strain by ratchet helix mutants. (A) Shown are the observed slow growth phenotypes of Mtr4 ratchet helix mutants. The R1030A displays the slowest growth out of the ratchet helix mutant residues. *mtr4-archless* is used as a slow growth control and D262A/E263A is the active site knockout. (B) Double mutants of the ratchet helix point mutations combined with an *archless* construct are displayed. *Archless* combined with either ratchet helix mutant results in synthetic lethality.

E1033A-*archless* were constructed, serially diluted, and tested for viability at 30ºC. Complementation with plasmid containing wild-type MTR4 was used as a positive control as well. Ratchet helix point mutants combined with archless affected cell growth in different ways. The *mtr4*-R1030A-*archless* mutant displayed synthetic lethality, while the *mtr4*-

E1033A-*archless* mutant displayed a slow growth phenotype (Figure 2-5). This result suggests a cooperative function of the arch and ratchet helix point mutants in RNA surveillance.

Mtr4 Arch Alone Does Not Affect Unwinding Activity or Sequence Specificity

The arch domain was first identified with the crystal structure of Mtr4. The only known activity of the arch is that it binds structured RNA and that it is required for proper 5.8S rRNA processing. It is known that the arch domain, when removed, does not affect the unwinding rates of wild-type Mtr4.[27] Interestingly, we have shown that the arch is not important for identifying a poly(A) sequence over a non(A) sequence, since we observed the same differentiation in rates on these substrates with the archless protein as we see with wild-type Mtr4 (Figure 2-6). However, when we combine either the R1030 or the E1033 ratchet

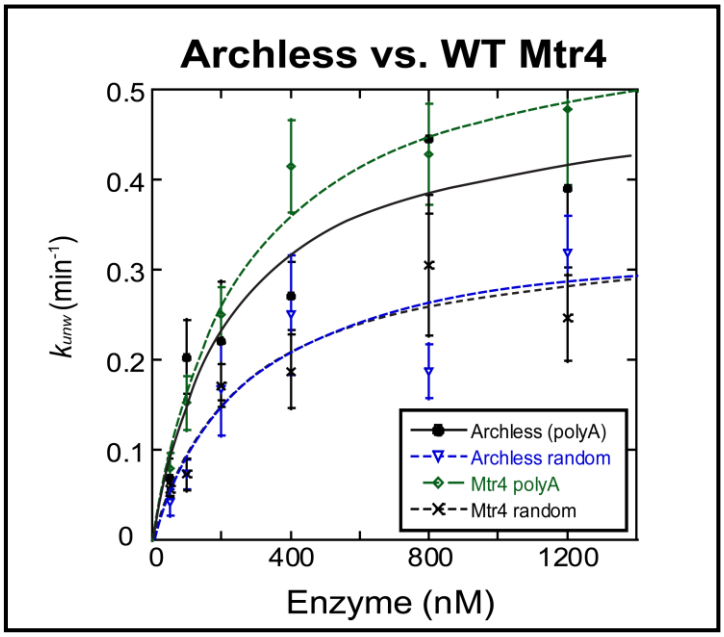

Figure 2-6. Archless and wild-type Mtr4 unwinding rates on a poly(A) and non(A) RNA substrate. Shown above are k_{unw} curves on a poly(A) substrate for Mtr4 wild-type (green) and archless (black); on a non(A) substrate for Mtr4 wild-type (black dashed) and archless (blue). Data show no significant differences in unwinding between wild-type and archless.

helix point mutant with archless, unwinding activity is abolished (Figure 2-7). It is only when we have this combination of ratchet helix point mutant and arch deletion that we observe no unwinding activity. Currently, the relationship between the arch and ratchet helix is unclear. This result suggests some cooperative function by the arch and ratchet helix of Mtr4 during interactions with RNA substrates involved in unwinding activity.

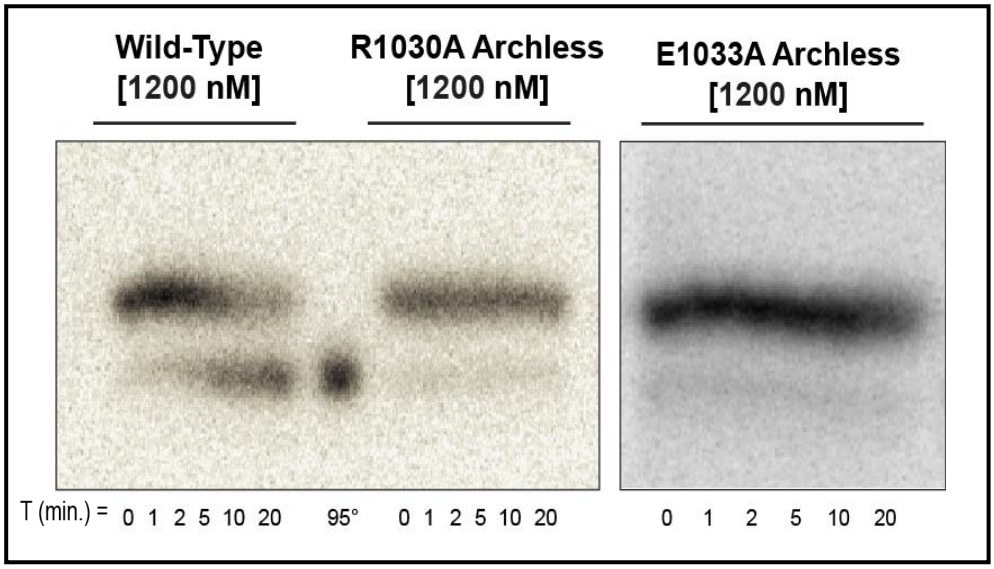

Figure 2-7. Unwinding assay on a poly(A) substrate with Archless combined with either R1030A or E1033A. A wild-type Mtr4 unwinding control shows strand displacement over time (far left). The R1030A-Archless (middle) and E1033A-Archless (far right) unwinding assay shows no displacement for either Mtr4 variant.

Effect of TRAMP Formation on Mtr4 Mutants

Since the observed *in vivo* effects of the Mtr4 mutants may be expected to arise through interactions in the TRAMP complex rather than Mtr4 alone, we decided to examine the Mtr4 mutants in the context of TRAMP. Trf4 and Air2 have been previously shown to stimulate the unwinding rate of wild-type Mtr4, increasing both the rate on a poly(A) and a non(A) substrate.[37] Preliminary results display a similar Trf4-Air2 dependent stimulation of

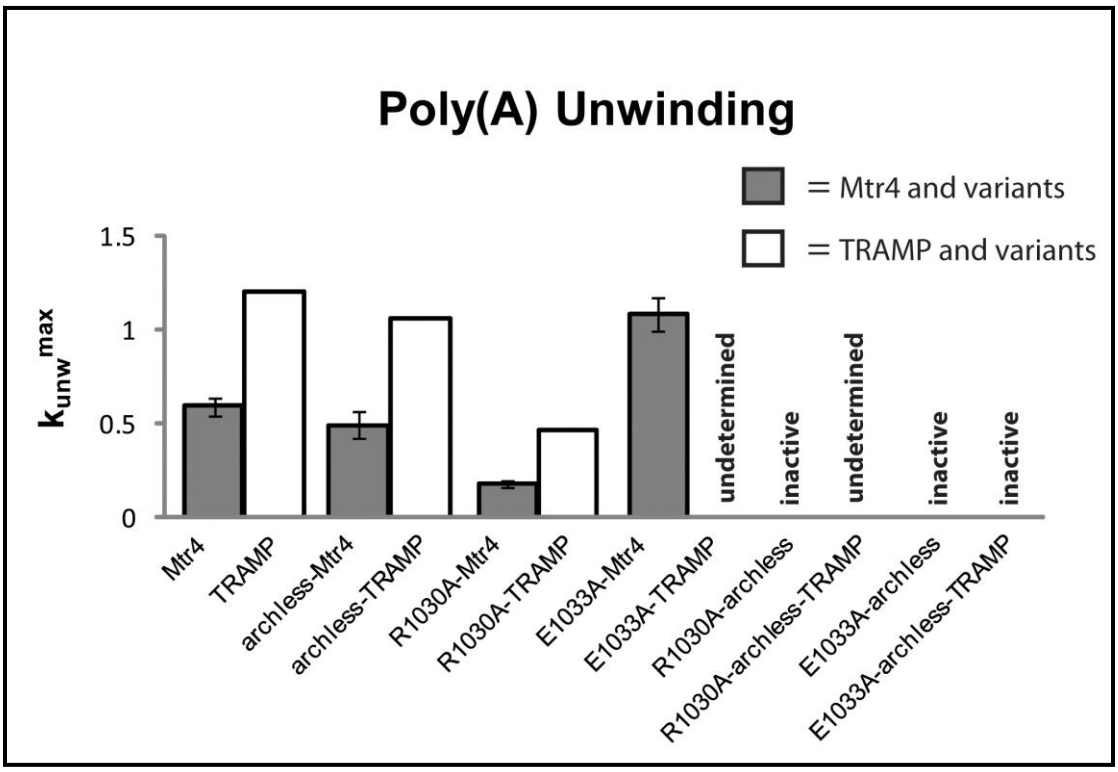

Figure 2-8. Poly(A) unwinding comparisons between Mtr4 mutants and TRAMP with Mtr4 mutants.

unwinding activity with R1030A, E1033A, and archless Mtr4 (Figure 2-8). We also observe the same relative effects on unwinding rate as observed with Mtr4 alone. Specifically, R1030A-TRAMP is ~2.5-fold slower than WT, E1033A-TRAMP appears faster, and no altered effect is observed for archless-TRAMP.

Surprisingly, R1030A-TRAMP regains the sequence specificity for a poly(A) substrate that was lost in Mtr4 alone (Figure 2-9). Thus, Trf4 and Air2 appear to have an effect on the ability of Mtr4 to recognize a poly(A) substrate. We are unable to determine activity of R1030A-archless-TRAMP due to poor solubility of the complex during purification. E1033A-archless-TRAMP, however, is well-behaved in solution and shows no unwinding activity. This loss of helicase activity is consistent with the *in vivo* data, suggesting that helicase activity is the essential function of Mtr4.

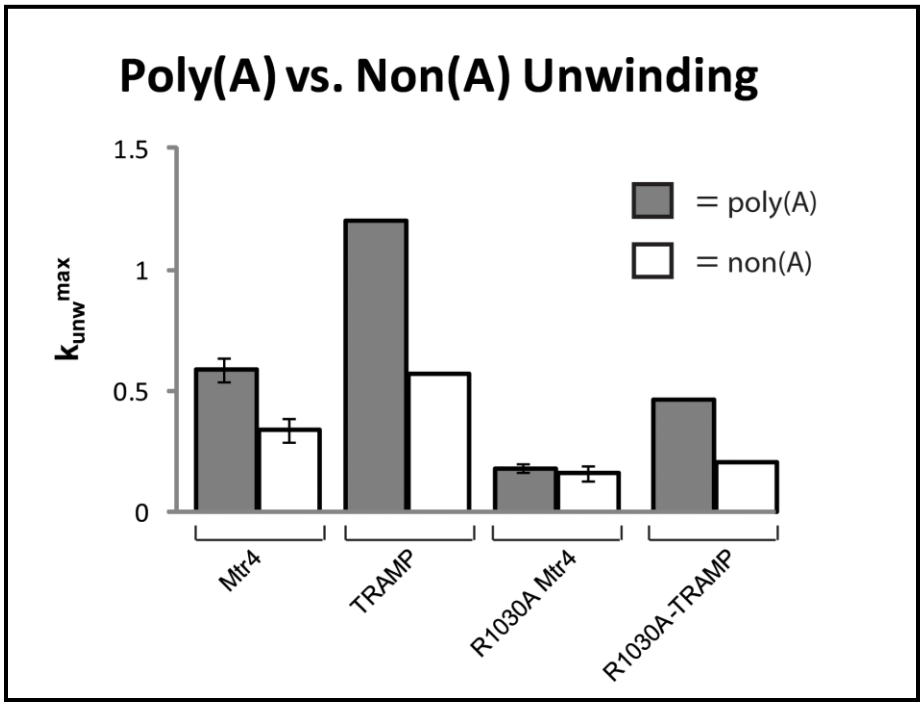

Figure 2-9. Unwinding activity of R1030A-Mtr4 versus R1030A-TRAMP on a poly(A) and non(A) substrate.

DISCUSSION/CONCLUSION

Conservation in the ratchet helix is observed to be more extensive in Mtr4 than in Hel308, hinting at expanded functionality such as sequence recognition. In Mtr4 the ratchet helix is highly conserved, even more so than other helicases in the Ski2-like family of helicases, suggesting an important role specific to Mtr4. The residue position 1033 on the ratchet helix of Mtr4 is strictly conserved throughout helicase types, and may have a similarly equivalent role in unwinding that W599 has in Hel308. When we mutate the glutamate at position 1033 to an alanine, unwinding activity increases. When the same residue is mutated to a tryptophan at position 1033 (to mimic Hel308), we observe slower unwinding activity. We were successful in targeting residues along the ratchet helix for mutational analysis, which furthered our understanding of the mechanism of unwinding and substrate recognition.

Residues along the ratchet helix of Mtr4 interacting with RNA bases is observed in the Mtr4-RNA bound structure. In the Hel308 DNA-bound structure, base stacking between the ratchet helix and unwound single stranded DNA is observed with Arginine 592 and Tryptophan 599. However, there are considerably more interactions in the Mtr4 RNA-bound structure with the RNA substrate than Hel308 with the DNA substrate. This observation raises the possibility that the ratchet helix may be involved in recognition of polyadenylated substrates. It is known that Mtr4 prefers a short 3' poly(A) tail around 5 nucleotides that is a product of Trf4 in the TRAMP complex. We have demonstrated that when Arginine 1030 is mutated to an alanine, Mtr4 loses the ability to distinguish between polyadenylated and non-polyadenylated substrates. Remarkably, poly(A) affinity is rescued when Mtr4 forms a complex with Trf4-Air2. Perhaps Trf4 and Air2 play a minor role in preferentially recruiting substrates for Mtr4 to unwind. Another possibility could be that the formation of the TRAMP complex (Trf4-Air2-Mtr4) causes a conformational change accommodating for the active site of Mtr4 to recognize sequence regardless of a single mutation that discriminates against poly(A) affinity. The R1030A mutation likely affects reading of a single nucleotide, suggesting that we have not disrupted the entire sequence reading interface of a 5 nucleotide poly(A) sequence. Trf4 has been shown to maintain an optimal adenylation range of 4-5 poly(A)s in sequential order.[36] Mtr4 plays a role in regulating this poly(A) addition by decreasing the rate of poly(A) after around 5 nucleotides. Since Mtr4 is known to have a binding interface of approximately 5 nucleotides, it is thought that Mtr4 latches on to the substrate at 5 poly(A)s and interferes with the Trf4 polyadenylation activity at that point.[20]

Mutation of ratchet helix residues R1030 and E1033 have different effects on unwinding activity. An R1030A mutation decreases unwinding activity while an E1033A mutation increases unwinding activity, suggesting that these residues may play distinct roles in the unwinding mechanism. Interestingly, an E1033W mutant (designed to mimic Hel308) decreases unwinding activity to R1030A levels, rather than increasing activity as seen in

E1033A. The glutamate at residue 1033 may act as a "gatekeeping" residue. When E1033 is mutated to an alanine, the diameter of the "RNA exit tunnel" is equivalent in size to the apo structure allowing more room for RNA to translocate through. When E1033 is mutated to a tryptophan, the tunnel is decreased by approximately 1.2 Å making a narrow exit for RNA to move through. Thus, it appears that the size or bulkiness of the residue at position 1033 plays a role in modulating unwinding activity. As with wild-type TRAMP, enhancement of unwinding activity was observed with all the Mtr4 mutants tested in the context of TRAMP. The Mtr4 mutants complexed with Trf4-Air2, though faster over all, still followed the same trends as the single mutations displayed on their own. Significantly, all of these mutants result in a slow growth phenotype, regardless of whether they increase or decrease unwinding activity *in vitro*. This data emphasizes the importance of the ratchet helix in acting as a finely tuned regulatory point critical for the proper function of Mtr4.

When analyzing the two structures of Mtr4, apo- versus RNA-bound, a noticeable shift in the ratchet helix is observed. When comparing the nucleic acid exit path the RNA-bound structure contains a significantly smaller tunnel than the apo structure. A shift of ~ 4.1 Å and an angle change of 3.76º occurs between the ratchet helix in the apo- and RNA-bound forms resulting in a narrower gap for the RNA exit tunnel.[22] From E1033 on the ratchet helix to S244 on an adjacent helix (representing the "RNA exit tunnel" diameter) in the RNA-bound form, a diameter distance is calculated at around 9.5 Å. Nucleic acid requires around 8-9 Å of movement from phosphate backbone to the outer atom of the base. Examination of the Mtr4 structures reveals a significant shift in the position of the ratchet helix. One interpretation of the structures is that they represent the difference between apo- and RNA-bound states. However, the position of the ratchet helix in the apo structure is identical to that in the apo- and DNA-bound structures of Hel308. An alternate explanation is that the RNA-bound Mtr4 structure represents a conformation for reading the 3' end only. Note that movement of the ratchet helix is associated with a partial closure or tightening of the "RNA

exit tunnel," which may impede passage of an RNA strand, but would still allow for reading of at least 5 nucleotides at the 3' end. In this model, the conformation observed in the apo structure may more closely resemble an active unwinding conformation. Structures of Mtr4 bound to longer substrates are needed to clarify this point that the ratchet helix may use multiple states from binding a substrate to unwinding.

Unexpectedly, we discovered arch domain involvement in Mtr4 unwinding. We have shown previously that archless alone has no observable effect on unwinding rate with the duplexed substrates tested.[27] However, when archless is combined with either ratchet helix mutant we lose the ability to unwind RNA substrates completely, regardless of whether the individual ratchet helix mutants cause an increase or decrease in unwinding activity. We discovered a combination in which we lose unwinding activity *in vitro* as well as observe synthetic lethality *in vivo*. This result suggests a role for the arch domain in unwinding activity which had previously been unrecognized. The reason for this could be explained by decreased stability of the protein, or by loss of substrate binding. Alternatively, the arch domain may play a more direct role in the Mtr4 unwinding mechanism. Although protein folding appears to be unaffected when the arch is removed, functional changes do occur. An *archless* construct of Mtr4 showed a defect in 5.8S + 30 rRNA processing.[27] We are also showing that an *archless* construct combined with a ratchet helix mutant causes cell death and loses unwinding activity. One explanation is that we have eliminated enough RNA-protein interactions to the point where Mtr4 can no longer bind a substrate, however further binding studies are needed to answer this question. The data presented here provide an initial framework for understanding the molecular details of the role of ratchet helix residues and the arch domain in RNA substrate targeting and unwinding.

CHAPTER 3

COMPREHENSIVE METHODS

ABSTRACT

Several techniques and methodologies were developed in order to characterize Mtr4 and TRAMP. Techniques include molecular cloning, mutagenesis, expression/growths, protein purification, *in vitro* transcription, radiolabeling and fluorescence labeling of nucleic acids, and RNA binding techniques using anisotropy and fluorescence correlation spectroscopy (FCS). A pertinent assay to develop was the use of fluorescently labeled RNA in characterizing Mtr4 binding affinities. In order to develop this method, RNA needed to be either transcribed *in vitro* or purchased. An efficient and reliable labeling procedure of RNA was then crucial to be able to use anisotropy, a more quantitative method for determining K_d's than electrophoretic mobility gel shift assays (EMSA), used previously. This chapter will include a detailed description of all the methods and techniques developed to further characterize the functionality of Mtr4, Mtr4 mutants, and TRAMP. Although some methods have been described in previous chapters, here will include a greater depth of information so future researchers will have all the tools necessary to successfully repeat all the experiments used for Mtr4 analysis.

INTRODUCTION

Mtr4 had already been recombinantly cloned, expressed, and purified in an *E. coli* expression system prior to my work on this project. The structure had previously been solved in the Johnson lab in 2010 as well. The Mtr4 structure provided us with the first RNA helicase in the Ski2-like family of helicases. A novel arch domain was identified that seemed to be involved in RNA processing of some substrates, but not essential for cell viability and

unwinding activities. When I took over this project, my objective was to characterize substrate recognition and unwinding by Mtr4 through mutational analysis testing the effects certain variants had on helicase activity and RNA binding. Analysis of the Mtr4 RNA-bound structure helped identify residues along the ratchet helix to potentially play a role in sequence recognition. Mtr4 mutant function was analyzed alone as well as in a TRAMP context. In the CONSTRUCT DESIGN section, full details of the plasmids used, the mutagenesis methods, and the expression methods employed are discussed.

TRAMP purification is a difficult task. TRAMP consists of three proteins that will dissociate if salt concentrations exceed 200 mM. This typically excludes any ion exchange chromatography techniques such as S (cation exchange), Q (anion exchange), and Heparin. Protocols for TRAMP purification have been tested previously, but the only way to purify active TRAMP was to use the Jankowsky lab protocol.[36] However, this protocol still had some kinks to work out through trial and error. In the PROTEIN PURIFICATION section, protocols for preparing active and pure Mtr4 mutants, and TRAMP are described in detail.

Mtr4 and TRAMP are involved in RNA surveillance processes, therefore necessitating the need to make RNA to be able to biochemically characterize how these proteins interact with RNA. It is expensive to buy large RNAs commercially, therefore a protocol to *in vitro* transcribe native RNA substrates of Mtr4 and TRAMP was essential. RNA substrates targeted for *in vitro* transcription included $tRNA^{iMet}$, rRNA such as 5.8S and 5.8S + 30, and snRNAs such as U4 and U6. Under the section *IN VITRO* TRANSCRIPTION, the procedure for transcribing RNA is detailed.

Methods of quantifying RNA typically require labeling reagents due to low concentrations of RNA and low sensitivity methods for detection of RNA alone. Such labels include (but are not limited to) fluorophores, radioisotopes, and biotin. For helicase assays, the standard method is through the use of ^{32}P labeled RNA, although there have been helicase assays that utilize the capabilities of fluorescence resonance energy transfer (FRET).

However, for accurate analysis of binding affinities the preferred method is anisotropy or fluorescence correlation spectroscopy (FCS). The utilization of efficient labeling techniques is crucial for our lab to perform the proper biochemical assays in characterizing RNA surveillance proteins. In the section 5' LABELING OF NUCLEIC ACIDS, detailed protocols for labeling the 5' end of transcribed RNA with either ^{32}P or a fluorophore are outlined.

In order to confidently calculate a K_d for Mtr4 and Mtr4 mutants with various RNA substrates, anisotropy and FCS were attempted. There was no standard pre-existing FCS protocol for monitoring protein-RNA interactions, however the want was there due to the real-time capabilities and numerous advantages for low level detection. Anisotropy is another standard method for measuring binding affinities. This method turned out to be more practical for use in Mtr4-RNA binding studies. Both methods required lots of effort in developing a reliable protocol for determining K_d calculations. In the sections ANISOTROPY and FLUORESCENCE CORRELATION SPECTROSCOPY the protocols for using these instruments and the tools for reproducing binding curves of Mtr4 binding to RNA substrates are described.

Characterization of the helicase and ATPase function of Mtr4 has been developed previously and elaborated on by several labs. The Jankowsky lab has taken the lead on developing TRAMP helicase assays and the Pyle lab has improved upon the ATPase assay of Mtr4 by malachite green. However, every lab is set-up differently and therefore modifications tend to be made to these established protocols. Mtr4, Mtr4 mutants, TRAMP, and TRAMP with Mtr4 mutants utilized these activity assay protocols with some slight modifications. Details of these newly revised methods are outlined in the sections HELICASE ASSAY and ATPASE ASSAY.

CONSTRUCT DESIGN

Using yeast genomic DNA (isolated from *S. cerevisiae*) as a template, various constructs of the desired proteins were created (mutants, truncations, etc.). Protein sequences containing introns are less frequent in this strain, therefore making *S. cerevisiae* easier to clone out of. Plasmids used for the desired constructs include pET 151-D-topo (Invitrogen), pRSFduet (novagen), Andy_pLC3, pET-15b (from the Jankowsky lab), and pETDuet for dual protein expression (novagen).

Mutagenesis

Point mutants of Mtr4 were made either using the QuikChange (Agilent) site directed mutagenesis procedure or a modified version of this QuickChange site directed mutagenesis procedure (known as the Megi Mutant Method). Both methods were employed simultaneously, and were the QuikChange procedure did not work the Megi Mutant Method typically did. The Megi Mutant Method uses primers that are designed to contain an overlapping region of 15-20 bp with a melting temperature between 40-60ºC. The non-overlapping region melting temperature should be 5-10ºC higher than the overlapping region.

Expression of Protein

All constructs used were recombinantly expressed in *E. coli* BL21-codon+-(DE3)-RIL cell line (Strategene). Wild-type Mtr4 was expressed using auto-induction in ZY media with proper antibiotics (ampicillin and chloramphenicol). Growths were incubated at 37°C for 6 hours and then transferred to room temperature shakers for 48 hours before harvesting. The Mtr4 mutants: R1030A, E1033A, R1030A/E1033A, E1033A-archless, and archless were expressed the same way as wild-type. The R1030A-archless double mutant was expressed using Super Broth (SB) media (a more enriched media than Luria Bertani). An overnight growth (25 mls) was used to inoculate a 500 ml SB growth and incubated at 37°C until an

OD_{600} of 0.6-0.8 was reached. Cells were then induced with 500 µls of 0.5 M Isopropyl β-D-1-thiogalactopyranoside (IPTG), final IPTG concentration of 0.5 mM, and moved to room temperature for 6-12 hours. Full length Trf4(D236A/D238A)/Air2 were expressed in a duet vector using Luria Bertani (LB) media. Starter cultures of Trf4(D236A/D238A)/Air2 were made in 8 mls of LB media with proper antibiotics (ampicillin and chloramphenicol), inoculated from a glycerol stock and incubated approximately 12 hours at 37ºC. These starter cultures were then transferred into 800 mls of LB with ampicillin and chloramphenicol, and incubated at 37ºC until they reached an OD_{600} of 0.6-0.8. At this point cells were induced with 800 µls of 0.5 M IPTG (or 0.5 mM IPTG final concentration). Cells were then incubated at 28ºC for 3-4 hours before harvesting. All cells were harvested (pelleted) at 8,000 rpm at 4ºC in a Sorvall SLC-4000 rotor and stored at -80ºC.

PROTEIN PURIFICATION

All protein constructs were lysed manually by chopping up the frozen pellet, followed by lysozyme treatment and a protease inhibitor cocktail of ~ 0.1 mg leupeptin, 0.1 mg pepstatin, and 14 mg phenylmethanesulfonylfluoride (PMSF). When necessary, arginine was added at 0.5 to 1.0 M to aid in solubility for the R1030A-archless mutant. Sonication followed after approximately 20 minutes of incubation with lysozyme treatment.

Mtr4

His-Mtr4, wild-type and mutants, were lysed with a 2X lysis buffer dilution, sonicated, and spun-down at 20,000 rpm's using a Sorvall SS-34 rotor. Protein was then purified using Ni affinity chromatography, heparin affinity, and gel filtration chromatography using a 320 ml superdex column. The final purification buffer off of gel filtration chromatography was 50 mM Hepes pH 7.5, 160 mM NaCl, 5% glycerol, and 2 mM β–ME.

TRAMP

His-Mtr4, His-Air2, and Trf4(D236A/D238A)-FLAG were purified together to make a 1:1:1 active TRAMP complex. His-Mtr4 was lysed with a 5x lysis buffer dilution and the co-expressed His-Air2 and Trf4(D236A/D238A)-FLAG were lysed with a 3 x lysis buffer dilution. Lysis buffer consisted of 50 mM NaH_2PO_4 pH 7.0, 250 mM NaCl, 10% glycerol, and 10 µM $ZnCl_2$. Pellets were lysed separately by sonication, and spun-down at 10,000 rpm using the Sorvall SS-34 rotor. Supernatants were combined on cobalt resin in the 4ºC room for 12-14 hours. Purification of the TRAMP complex was carried out in the 4ºC room throughout, until storage at -80ºC (complex is unstable outside of 4ºC). Complex was then washed with 100 mls lysis buffer with an additional 20 mM imidazole. Elution buffer was then incubated on cobalt resin while shaking for 5-10 minutes before collecting fractions. The elution buffer consisted of 50 mM NaH_2PO_4 pH 7.0, 200 mM NaCl, 10% glycerol, and 10 µM $ZnCl_2$. All fractions were typically used (verification through SDS-PAGE gel) and concentrated to ~ 4 mls for further incubation on FLAG resin.

Complex was incubated on FLAG resin for 2 hours at 4ºC with 1 ml of sample per ~ 250 µls resin. The sample was thoroughly washed with 1 ml wash buffer 3x with 10 minute incubations on the FLAG resin. FLAG and NAP-25 wash buffer contained 50 mM NaH_2PO_4 pH 7.0, 200 mM NaCl, 10% glycerol, and 10 µM $ZnCl_2$. A swinging bucket centrifuge was used to pellet resin between washes, spinning at 1000 x g for 5 minutes in the 4ºC cold room. The TRAMP complex was then eluted off of FLAG (in a 1:1:1 ratio) with elution buffer consisting of wash buffer components, plus 100 µg/ml FLAG peptide. First elution was 500 µls for 20-30 minutes of incubation, second and third elutions were 250 µls for 20 minute incubations. All elutions were spun down at 1000 x g for 5 minutes, and decanted off into a 1.5 ml microcentrifuge tube. Elutions containing TRAMP (typically all 3), were concentrated to 2.5 mls and used for further purification over a NAP-25 column.

NAP-25 columns are pre-packed Sephadex G-25 sizing columns from General

Electric (GE) used for small scale purification. Equilibration of 25 mls of wash buffer is sufficient for NAP-25 before use. If using a used NAP-25 column, wash with ~5-6 column volumes of water to rinse out any residual ethanol. Sample is fully loaded (by gravity flow) onto the NAP-25 column before adding 5-6 mls wash buffer to follow after sample. Elutions were immediately collected in 0.5 ml fractions for up to 8 fractions by gravity flow. TRAMP complex typically elutes in the first 6 fractions, and is then concentrated to ~ 200 µls and flash frozen with liquid nitrogen in 20 µl aliquots. All tubes used to store TRAMP and TRAMP mutants have been previously autoclaved to avoid RNase contamination. Gloves must be used at all times when dealing with this protein complex.

Finally a BSA concentration gradient was used to calculate the concentration of TRAMP. Since there are three protein components in the TRAMP complex, concentration determination for helicase activity purposes was solely based upon the amount of Mtr4 present. Therefore a TRAMP sample along with a BSA concentration gradient of 0.4, 0.2, 0.1, and 0.05 mg/ml was run on a gel and intensities were calculated based on densitometry. Gels were quantified using multigauge software by Fuji Photo Film Company, and a standard

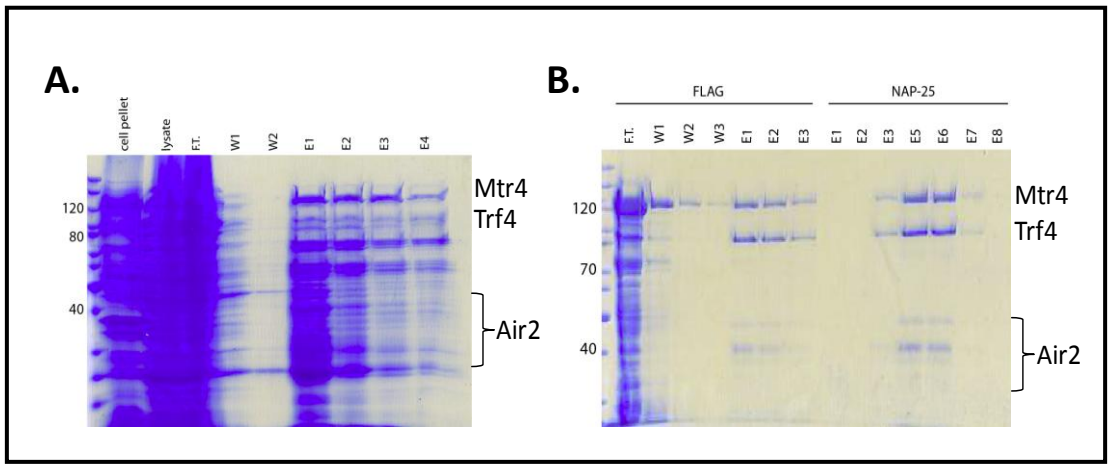

Figure 3-1. TRAMP prep SDS-PAGE gels. To the left (A) is TRAMP post cobalt resin, and on the right (B) is TRAMP post FLAG resin and post NAP-25 column.

curve was graphed of the BSA concentrations. Using the BSA standard curve equation, and the band intensity of Mtr4, TRAMP concentrations were calculated. BSA samples were made from a 10 mg/ml stock purchased from New England Biolabs and diluted in the same phosphate buffer TRAMP was prepped in. Gel figures throughout the TRAMP preps are displayed below in Figure 3-1.

IN VITRO TRANSCRIPTION

Master mixes of 5 mls (in a 15 ml conical; vortex) for tRNA-DNA PCR with aliquots of 160 µls will give a workable stock. Outline of PCR components and concentrations are listed in Table 3-1 and cycle parameters in Table 3-2. The PCR should be at a concentration of ~ 1000 ng/µl when blanking with water.

Table 3-1: PCR reaction set-up (5 ml reaction)

Component	Concentration	Volume	Notes
*DNA (from PCR rxn)	0.4 ng	21.3 µls	Stock DNA at 93 ng/µl (0.4 ng/ul final)
forward primer	1 M	48 µls	Stock at 1378.4 ng/µl (MW=13,245.6)
reverse primer	1 M	37.5 µls	Stock at 1269.9 ng/µl (MW=9,544.2)
H_2O		4193.2 µls	
dNTP	2 mM	100 µls	100 mM stock mixture of dNTP's
10X Pfu buffer	1X	500 µls	
Pfu (1:300)	diluted Pfu	100 µls	Johnson lab prepped stock

After each PCR reaction, set aside one tube of PCR product (that you have confirmed has worked) and PCR clean-up to use as your template DNA for the next PCR reaction. The original tRNA DNA template stock is archived as SJJ 041.

Table 3-2: Cycle parameters		
1X	95°C	2 min.
30X	95°C	30 sec.
	64°C	30 sec.
	72°C	1.5 min.
1x	72°C	3 min.
1x	4°C	∞

Transcription reactions are to be conducted in an autoclaved 1.5 ml microcentrifuge tube, containing a maximum volume of 1 ml per tube. If preparing a 5 ml transcription reaction one would setup 5 - 1 ml reactions in 1.5 ml microcentrifuge tubes. Transcription reagents are listed below in Table 3-3.

Table 3-3. 1 ml Transcription reaction (add in the following order)			
	Volume	**Final Concentration**	**Notes**
H_2O	600 µls		
10X Buffer	100 µls	1X	
DNA Template	80 µls	8% volume	PCR Product (no PCR clean-up necessary)
NTP's			
U	40 µls	4 mM	Stock made at a conc. of 100mM
A	40 µls	4 mM	Stock made at a conc. of 100mM
G	40 µls	4 mM	Stock made at a conc. of 100mM
C	40 µls	4 mM	Stock made at a conc. of 100mM
GMP	40 µls	16 mM	Stock made at a conc. of 200mM
T7 polymerase	20 µls	To be optimized	Use 1000X stock

Once all of the transcription reaction reagents have been added, incubate at 42°C in a water bath for 3 hours. Precipitation should be visible within an hour from the start of the transcription reaction. This precipitate is magnesium pyrophosphate salt, and optimization of whether more $MgCl_2$ should be added as well as T7 needs to be done for each new RNA substrate.

After incubation of the transcription reaction, the precipitated pyrophosphates are spun down at 5,000 rpm for 30 seconds. Supernatant is then loaded onto a sizing column and

fractions are run on a RNA denaturing gel. Fractions containing desired RNA are then pooled and stored away at -80ºC for future use. Concentration can be determined by using a NanoDrop spectrophotometer (Thermo Fisher), and calculated in µM by the following equation:

$$[\text{RNA}]\mu M = \left[\frac{ng}{\mu l} * (\frac{1}{1.4}) * \frac{\text{mole}}{g} * \frac{\text{g}}{10^9\text{ng}} * \frac{10^6\mu\text{l}}{L}\right] * \frac{10^6\mu\text{moles}}{\text{mole}}$$

10X Transcription reaction buffer consisted of 400 mM Tris pH 8.0, 240 mM $MgCl_2$, 10 mM spermidine, 50 mM dithiothreitol, and 0.1% triton X-100. tRNA Sizing Buffer consisted of 50 mM Tris pH 7.5, 160 mM NaCl, 24 mM $MgCl_2$, 2 mM β–ME, and 5% glycerol. RNA 8% Denaturing Gels were made by adding 14 g urea (microwave in 5 mls water for 20 seconds), 3 mls 10X TBE, 6 mls 40% acrylamide, 99.6 µls 30% APS, and 12 µls TEMED in a total of 30 mls final volume to make 3 gels at a time. 10X TBE buffer was made with 890 mM Tris base, 890 mM boric acid, and 20 mM EDTA with a pH of 8.0. 10X Pfu buffer consisted of 200 mM Hepes pH 8.6, 10 mM $(NH_4)_2SO_4$, 100 mM KCl, 0.1% triton X-100, and 20 mM $MgSO_4$.

5’ LABELING OF NUCLEIC ACIDS

Radiolabeling *in vitro* Transcribed RNAs

After transcription and purification of the desired RNA, a 5’- [^{32}P] - phosphate is attached. In order to radiolabel *in vitro* transcribed RNAs, the 5’ end must be dephosphorylated in a phosphatase reaction using 1 µl calf alkaline phosphatase (purchased) per 10 µl reaction. The reaction was incubated at 37ºC in a 0.65 ml autoclaved microcentrifuge tube for 1.5 hours. The phosphatase removal reagent was then added (10 µls) and incubated at room temperature for three minutes with constant agitation to

precipitate the phosphatase enzyme. The precipitated phosphatase was spun-down and the sample was transferred to a new, autoclaved 0.65 ml microcentrifuge tube before proceeding to be phosphorylated with the γ-^{32}P-ATP.

Using T4 polynucleotide kinase (~ 1-2 µls per 20 µl reaction), the RNA was incubated at 37ºC in the Hevel lab designated water bath for ^{32}P with 1 µl of 6000 Ci/mmol, 150 mCi/ml ^{32}P for 3-4 hours. A native PAGE gel was then run at 100 volts for 90 minutes to separate the desired radiolabeled RNA from free γ-^{32}P-ATP. The RNA gel was exposed to Kodak film for ~ 1 minute and then developed in developer solution (Kodak, dilute 103 mls in 370 mls of water). A dye line is apparent in visible light and can be used as a marker outline to trace on the film. The Kodak film was then used to place over the radioactive gel to trace where the desired radiolabeled RNA band to gel extract was.

A razor blade was then used to cut out the band. The gel band with the radiolabeled RNA was then incubated overnight in 400 µls of gel extraction solution containing 0.5 M ammonium acetate, 0.1 M EDTA, and 0.1% sodium dodecyl sulfate (SDS). The sample was then taken out the following morning and ethanol precipitated with the addition of 1 µl of 20 µg/µl glycogen (a carrier molecule), and 3 times the volume of chilled ethanol was then added. This was stored at -80ºC for 20 minutes before spinning down at 4ºC for twenty-five minutes. All liquid was decanted off and the precipitated pellet of RNA was left open to dry in the fume hood for at least 2-4 hours before bringing up in desired volume with water.

Gel Electrophoretic Mobility Shift Assay (EMSA)

In order to obtain rough binding affinities for Mtr4 with potential RNA substrates, an EMSA assay was utilized. Using radiolabeled RNA substrates at a concentration well below K_d range, concentrations of protein were varied and incubated for 30 minutes at 30ºC (yeast proteins) in a suitable binding buffer (differs amongst proteins). For Mtr4, a buffer consisting of 20 mM Tris pH 8.0, 5 mM $MgCl_2$, 50 mM KCl, 2 mM DTT, and 100 µg/ml BSA was

used. The different concentrations of protein with RNA were then ran on a native PAGE gel and exposed to X-ray film to qualitatively calculate a dissociation constant from gel shifts (phosphorimager is now available as well). The larger the complex (bound or not), the higher up in the gel the band would appear. Sometimes the native gel would have to be run at a higher voltage (~140 volts) to get some of the more positively charged proteins to enter. The gels are then quantified using multigauge software, and fit to the Hill equation; fraction bound = $1/(1 + K_d^n/[P]^n)$. Where fraction bound = $1 - ([RNA]_{free}/[RNA]_{total})$.

5'-Fluorescence Labeling of Nucleic Acids

Thiol chemistry was utilized to label RNA substrates with a 5'-fluorescent tag. If the RNA had been *in vitro* transcribed, then a dephosphorylation step was necessary using alkaline phosphatase at 37ºC for one hour (same as described for ^{32}P labeling). If RNA was purchased commercially, the dephosphorylation step was not needed. ATP-γ-S at a final concentration of 2.5 mM was then added with T4 polynucleotide kinase at 37ºC for one hour to replace the 5'-phosphate with a terminal phosphate containing a double-bonded sulfur (instead of a terminal oxygen). The alkaline phosphatase is incapable of removing this γ-S phosphate, relinquishing an inactivation step before the kinase reaction. A fluorescent maleimide was then added to react with the sulfur on the 5'-phosphate at 65ºC for one hour. Fluorescein maleimide and Alexa Fluor 633 C5-maleimide have been successfully used for 5' RNA labeling with this method. Purification of the labeled RNA from free fluorescent dye was achieved through the use of a 24 ml Superdex 200 column monitoring simultaneous peak readings at 254 nm for RNA and the absorbance wavelength for the fluorescent tag used. Ethanol precipitation (as previously described for ^{32}P labeling) was performed on the fractions containing the correctly labeled RNA substrate, allowing for re-suspension of the RNA in smaller volumes (~ 10 µls).

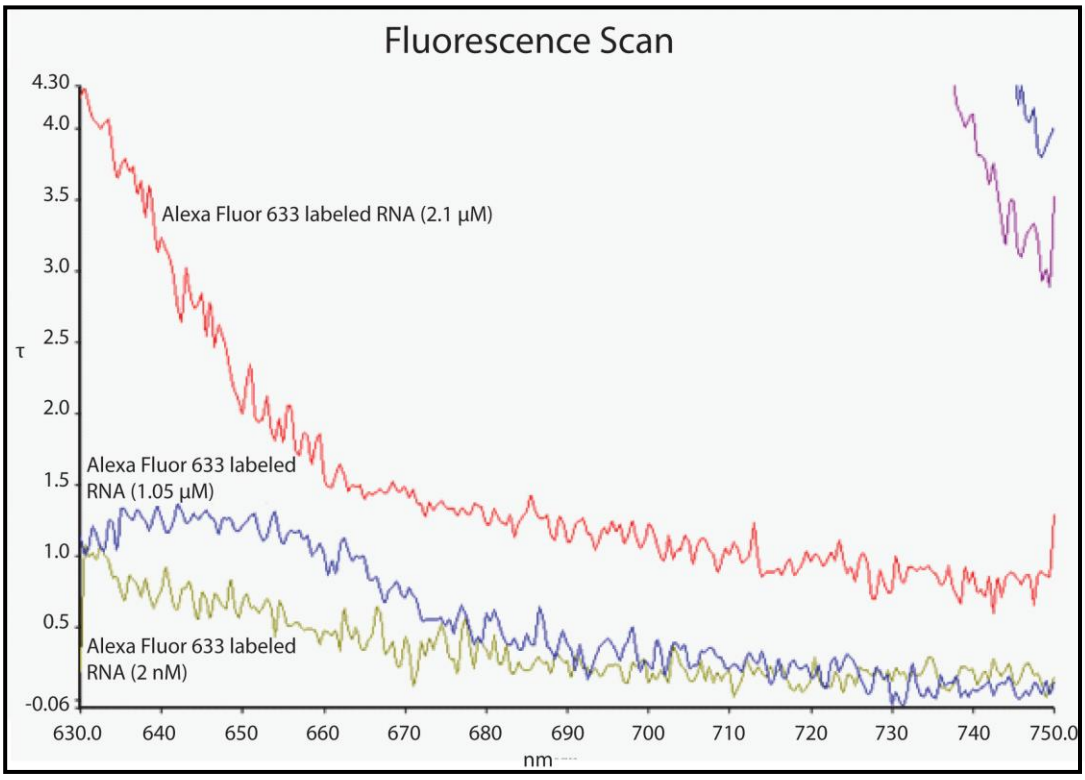

Figure 3-2. Fluorescence scan detecting different forms of the Alexa Fluor 633 dye. Zoomed in view of low concentrations of a duplex RNA strand 5' labeled with the A.F. 633 dye.

Testing the Quality of Fluorescently Labeled RNA Substrates for F.C.S.

Using the fluorimeter in the Chen lab, a scan was setup to read wavelengths from 630 nm to 750 nm, with an excitation of 610 nm.

- Excitation slit set to 10 (nm)
- Emission slit set to 10 (nm)
- Scan speed (nm/min) set to 100

Examples of usable concentrations are shown in Figures 3-2 and 3-3 (note that the 2.1 µM sample was too concentrated for the FCS and was therefore diluted).

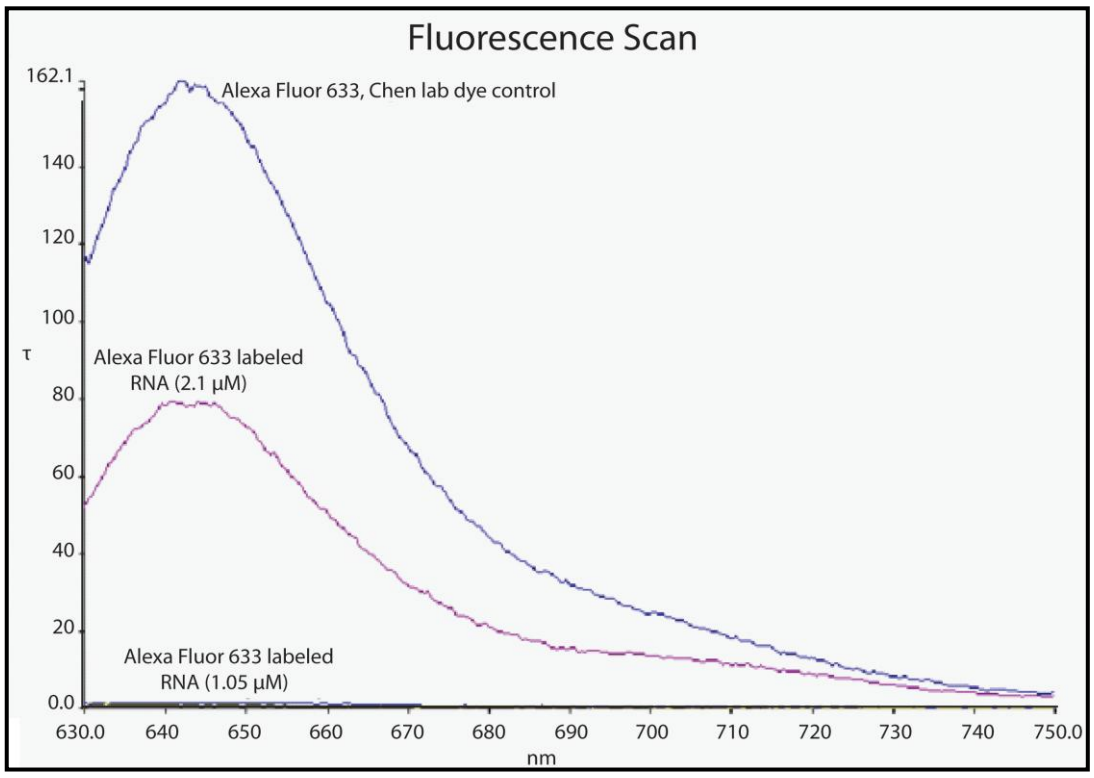

Figure 3-3. Fluorescence scan detecting different forms of the Alexa Fluor 633 dye. Free dye signal of the A.F. 633 versus the lower concentrations of RNA labeled with A.F. 633.

ANISOTROPY

Fluorescence polarization was used to assess binding for protein-protein and protein-RNA complexes. Samples using Alexa Fluor 633 C5-maleimide or Fluorescein maleimide dye to label RNA (as outlined in the 5'-fluorescence labeling of nucleic acids section) or smaller proteins containing free cysteines can be used for anisotropy. The polarized light emitted from the fluorescent dye gives an anisotropic value, r(t). This value is a measure of the average angular displacement of the fluorescent dye, with a lower value indicating isotropic diffusion and a higher value indicating a more restricted compound (typically suggests the occurrence of binding). Therefore, data collection needs to be obtained with the excitation lens set to vertical polarization at all times, and the emission lens collected at both a vertical and horizontal polarization to calculate the anisotropy value for a given sample.

In much the same way as an EMSA, concentration of the fluorescently labeled substrate was held consistent at a concentration below the K_d. Then concentration of protein was gradually increased from 0 to a high enough concentration to reach binding saturation (trial and error). With the Mtr4 and Trf5 fluorescein labeled peptide, saturation was reached at a concentration between 1.5-8 µM of Mtr4. With Mtr4 and RNA binding assays, concentrations varied depending on RNA substrate used and whether it was an Mtr4 mutant or wild-type. The Synergy H4 Hybrid Multi-Mode Microplate Reader from BioTek (located in the Dickenson Lab) has the capabilities of measuring fluorescence polarization in a 96- or 384-well plate, saving on time and reagents. When setting up the experiment in the Dickenson lab, an optimal intensity is achieved in the range of 1000 - 5000 using a tungsten light source, with a gain value as low as reasonable. The gain value is an additional amplification of voltage to increase signal when concentrations are low, however the error tends to increase with increased gain. Sigmaplot software was used for curve analysis and K_d determination.

FLUORESCENCE CORRELATION SPECTROSCOPY

This is a useful technique to measure transient interactions and precise real-time binding constants amongst complex forming protein-ligands. A water emersion microscope slide was created by adding a drop of water to the side that comes in direct contact with the lens, and 15 µls of sample to the top of the slide. The laser was then positioned to directly hit the fluorescent sample by adjusting the microscope slide. Once the sample was centered, the lights were turned off in the room to allow for the specified laser's power source to be turned on. The power supply was set at 5 volts and 0.5 amps for current. The program used to run the experiment is called ALV correlator. Initial readings of 400-500 Hz for the frequency should be observed using the ALV correlator. In order to detect particles passing

(incorporating spikes that ruin the data) or photobleaching, at least 3 measurements are taken for the same sample. Initial experiments using F.C.S. have been with Mtr4 (wild-type) and

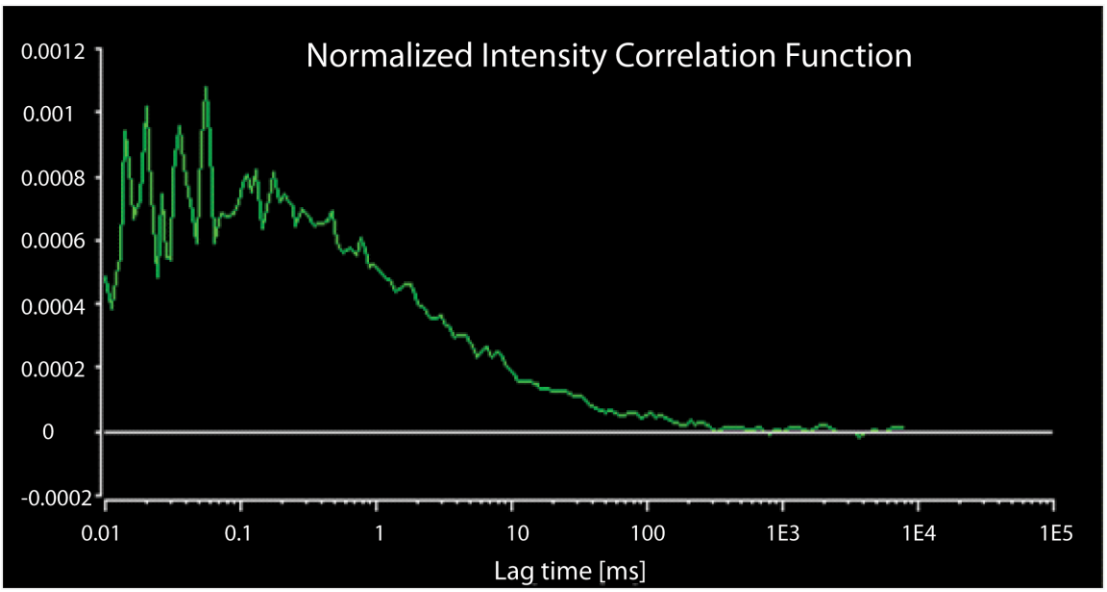

Figure 3-4. Fluorescence correlation curve of Mtr4 bound to 5' A.F. 633 labeled duplex poly(A) RNA.

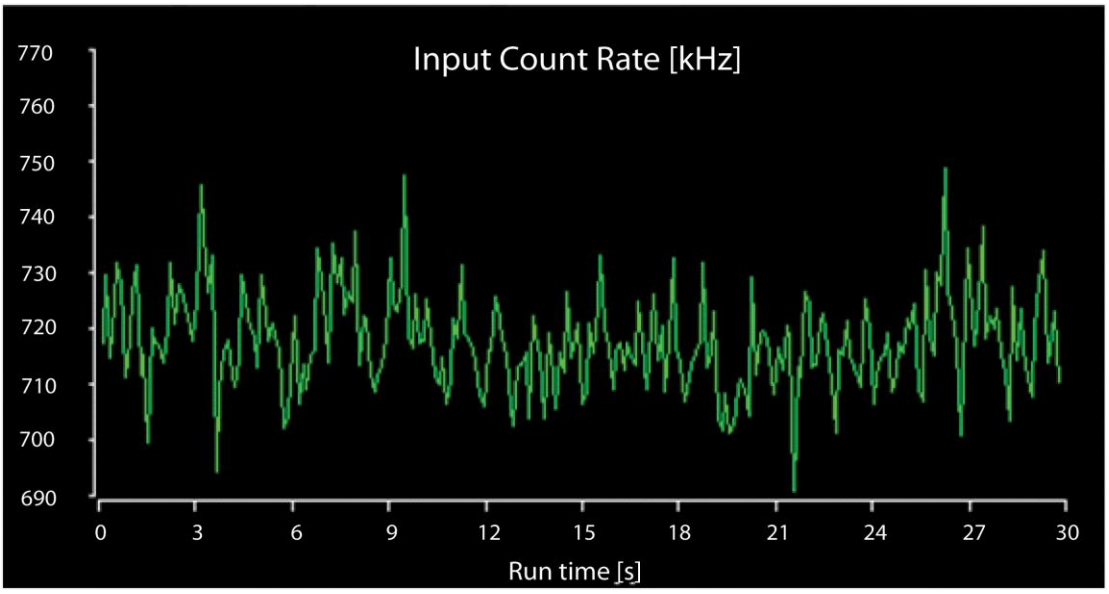

Figure 3-5. Input count rate of the variation in fluorescence of Mtr4 bound to 5' A.F. 633 labeled duplex poly(A) RNA.

the ratchet helix mutants, testing binding to the poly(A) versus non(A) RNA duplex with a 5' Alexa Fluor 633 label. Results have shown binding does take place, and calculated dissociation constants have been calculated. The disadvantage to this technique has been the software and calculations used for K_d measurements.

HELICASE ASSAY

A radiolabeled 16 nucleotide top strand was displaced over time when incubated with Mtr4 or TRAMP and saturating levels of ATP. Reactions were carried out at 30°C in a controlled water bath. The buffer used was 40 mM MOPS pH 6.5, 100 mM NaCl, 0.5 mM $MgCl_2$, 5% glycerol, 0.01% NP-40 substitute, 2 mM DTT, and 1 U/µl of Ribolock (Thermo Fisher). Reactions were allowed to incubate for 5 minutes with ~ 0.2 nM RNA (final concentration) and the indicated concentration of Mtr4, Mtr4 mutant, TRAMP, or TRAMP with Mtr4 mutant protein.

Reactions were initiated by the addition of equimolar ATP and $MgCl_2$ at a final concentration of 2 mM. At specified time points, aliquots of the reaction were removed and quenched at a 1:1 ratio with buffer containing 1% SDS, 5 mM EDTA, 20% glycerol, 0.1% bromophenol blue and 0.1% xylene cyanol. For Mtr4 helicase assays, concentrations at 1200, 800, 400, 200, 100, and 50 nM were tested. Samples were taken at time points of 0, 1, 2, 5, 10, and 20 minutes for the higher concentrations (1200, 800, and 400 nM), and 0, 1, 4, 10, 20, and 60 minutes for the lower concentrations (200, 100, and 50 nM). For TRAMP helicase assays, concentrations at 400, 200, 150, 100, 75, and 25 nM were tested. Samples were taken at time points of 0, 1, 2, 5, 10, and 20 minutes for the higher concentrations (400, 200, and 150 nM), and 0, 1, 4, 10, 20, and 60 minutes for the lower concentrations (100, 75, and 25 nM). Aliquots were run on a native 15% TBE polyacrylamide gel at 100 V for 115 minutes.

Radioactivity was visualized as performed using film or phosphor screen. Gels were wrapped in cellophane prior to exposure. Film was developed and then quantified using

multi-gauge software. Calculations of the observed rate constants (k_{unw}), and amplitudes (A) were performed using integrated first-order rate law. Curve fits were made to data collected in triplicate, Figure 3 (Fraction unwound = $A(1-\exp(-k_{unw}\cdot t))$(31,32,50). The k_{unw}^{max} and $K_{1/2}$ values were calculated using best fit curves as done in (31), with the equation, $k_{unw}= k_{unw}^{max}, {}_{E}$ $[E]/[E] + K_{1/2}, {}_{E}$, where [E] is enzyme concentration, $K_{1/2}$ is functional affinity and $k_{unw}^{max},{}_{E}$ is the unwinding rate constant at enzyme saturation.

RNA Substrates Used for Helicase Assay

The RNA substrates were designed to mimic unwinding substrates used in the recent study by Jia et al.[36] Two 22 nucleotide ssRNAs (bottom strand), and two 41 nucleotide ssRNAs (bottom strand) (each with a unique 3' end) were incubated independently with a complementary 16 nucleotide ssRNA (top strand) at 95°C for 10 minutes after which samples were slowly annealed to room temperature.

The 16 nucleotide top strand was labeled with γ-^{32}P ATP and T4 polynucleotide kinase and quenched by heating to 95°C before annealing. The RNA substrates were purified by native PAGE, gel extraction and ethanol precipitation. All RNAs used in this study were purchased from Integrated DNA Technologies (IDT). The substrate sequences are as follows with duplex regions underlined:

R16 (top strand of all three substrates) = 5'<u>AGCACCGUAAAGACGC</u>3',

R22A (poly(A) overhang) = 5'<u>GCGUCUUUACGGUGCU</u>UAAAAA3',

R22R (non(A) overhang) = 5'<u>GCGUCUUUACGGUGCU</u>UGCCUG3',

R41A (poly(A) overhang) =

5'GCGUCUUUACGGUGCUUAAAACAAAACAAAACAAAACAAAA3',

R41R (non(A) overhang) =

5'GCGUCUUUACGGUGCUUGCCUGUUCGUGUCCUGUUGCUGCU3'.

ATPASE ACTIVITY

To test for the activity of Mtr4 hydrolysis of ATP, a malachite green assay modified from Bernstein et al. was used. Using a plate reader, absorbance was monitored at 650 nm with a VERSA max tunable plate reader (Molecular Devices). An increase in absorbance at 650 nm correlates to free inorganic phosphate and therefore increased ATP hydrolysis. A colorimetric malachite green assay, adapted from Bernstein et al,[20] was modified based on the Pyle lab's protocol.[82] The malachite green solution was made in a 2 x concentration. For 500 mls, 0.15 g of malachite green oxalate, 1 g of sodium molybdate, and 0.25 mls Triton X-100 were added to a mixture of 0.7 M HCl and left to stir for 1 hour at room temperature. Once the solution was mixed fully, it was covered in foil to protect from light and stored at 4°C for up to 6 months. The reactions setup contained 25 mM Tris pH 7.5, 10 mM Mg Acetate, 2 mM β-mercaptoethanol, 0.5 μM of protein, and 0.2 μM of RNA (for Mtr4 ratchet helix mutants we used the same dsRNA used in the helicase assays with the short poly(A) tail). The reactions were initiated with the addition of 2 mM ATP and time points were taken at 0, 5, 10, 15, 20, and 30 minutes. A 5 x quenching solution (250 mM EDTA) was then mixed with each sample to reach a final concentration of 50 mM EDTA. The 2 x malachite green solution was then diluted to 1 x and added in a 9:1 excess to the sample to let sit for 30 minutes to complete the reaction before reading the absorbance at 650 nm. The instantaneous reaction rate ([Pi] μM min -1) was calculated by fitting a linear trend line to the absorbance values of time points using KaleidaGraph software. To determine the enhancement of RNA on Mtr4 and Mtr4-archless activity, reactions without RNA were used to obtain background values.

CONCLUSIONS

Within this chapter are the techniques and methods used for biochemical characterization of Mtr4. This should provide all future researchers with the proper tools to

be able to study Mtr4 extensively. Detailed methods including the molecular cloning techniques, protein expression, and protein/complex purifications are outlined. Several improvements in methods such as the helicase assay, the ATPase assay, and *in vitro* transcription of RNA are included. Additional techniques (included in this chapter) for labeling nucleic acids with ^{32}P and fluorophores allowed for studies using anisotropy and FCS for more accurate measurements of binding affinities. This chapter provides an archive of the studies that have been achieved characterizing the RNA helicase Mtr4, and aims to act as a guideline for future research methods to be employed on RNA surveillance proteins.

CHAPTER 4

SUMMARY AND FUTURE DIRECTIONS

REVIEW AND FUTURE DIRECTIONS

RNA regulation is an important process, yet little is known as to how the proteins involved function at the mechanistic level. The focus throughout this thesis has been on the RNA helicase Mtr4 involved in RNA surveillance. The lack of understanding in mechanistic detail of unwinding functionality and substrate recognition has been the key focus. Previous literature had hinted that the slight differences in ratchet helix between Mtr4 and the Ski2-like DNA helicase Hel308 could explain their functional differences, such as substrate preferences. Mutational analysis along this ratchet helix revealed differing effects on unwinding activity depending on the residue position mutated (Chapter 2). The R1030A mutation slowed unwinding rates and inhibited poly(A) preferential unwinding, while E1033A increased unwinding rates (Chapter 2). When either one of the ratchet helix mutants were combined with an *archless* construct, unwinding activity was abolished *in vitro* and synthetic lethality was observed *in vivo* (Chapter 2). This provided insight into the residues involved in substrate recognition and unwinding rates, as well as identified a new function for the arch domain of Mtr4. Below is an outline for future directions of outstanding questions about Mtr4 and the binding partners it interacts with.

TRF5-MTR4 STRUCTURAL AND MUTAGENESIS STUDIES

With the aid of anisotropy we have identified a small 27 residue fragment of Trf5 that directly interacts with full-length Mtr4 and archless-Mtr4 *in vitro*. Our collaborators in the van Hoof lab had previously identified residues 98-124 of Trf5 (by yeast two-hybrid experiments) to show an interaction with Mtr4 and archless. In Figure 4-1, the initial results of the Trf5 fluorescein labeled peptide binding to Mtr4 at varying concentrations of protein

show a rough dissociation constant of about 10 µM, using Sigmaplot software. This is the first result showing that Trf5 binds Mtr4 without the aid of the Air proteins. From here we can try truncations of the Trf5 peptide from the N- and C-terminus and test binding further to identify an even smaller portion of Trf5 required for interaction with Mtr4. With the affirmation of binding through anisotropy, we can try co-crystallization trials with the commercially purchased peptide of Trf5 and full-length or other smaller truncations of Mtr4 (which has been crystallized before). First attempts would require purification of the desired Mtr4 constructs mixed with an excess of Trf5 peptide (with >98% purity) prior to setting up robot trays. If no crystals result from that, further trials will proceed with the potential for soaking the peptide into a pre-existing Mtr4 crystal.

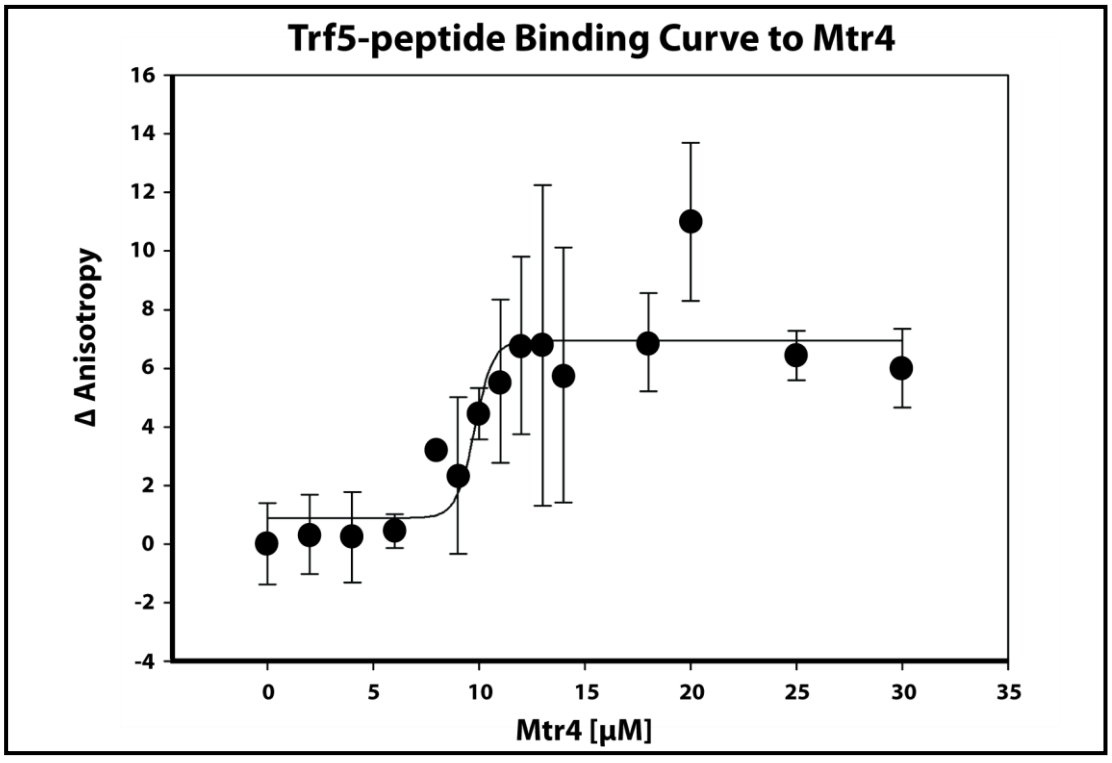

Figure 4-1. Binding curve of Mtr4 full-length to a Trf5 peptide. Change in anisotropy value is plotted versus change in concentration of Mtr4.

Winged Helix, Domains 1 & 2

Further analysis may include anisotropy tests of different domains of Mtr4 to identify a minimal region of Mtr4 that binds to Trf5. These results would lead to crystallization trials as well with such combinations as the core domains 1 & 2 of Mtr4, or just domain 3 (the winged helix) combined with the Trf5 peptide. All of these constructs have been successfully cloned, and just need to be purified for use in anisotropy experiments. If an apparent K_d is measured and it is within range of the K_d measured for full length and archless Mtr4, then crystallization trials will be attempted in the same manner as described in the previous section.

Trf5 Peptide Fragments: Finding a Minimal Binding Region to Mtr4

A small region of Trf5 (27 residues) has been shown to bind Mtr4. However, it is unclear if all these residues are needed for this interaction. Based on the secondary structure prediction of the Trf5 peptide sequence (Figure 4-2) there appears to be a β–strand and α–helix contributing to the structure, based on psipred server predictions. In the absence of a structure, truncation mutants would be beneficial in order to determine the absolute minimal binding region of Trf5 necessary to bind Mtr4. A possible truncation would be to delete the first 8 residues and test if it is the predicted structured region that binds Mtr4 by anisotropy techniques. Since it is thought that both Trf5 and Trf4 interact with Mtr4 in a similar manner (due to their sequence homology), a sequence alignment was produced revealing conserved residues potentially important for this binding interaction (Figure 4-2). Using the information gained through truncation mutant binding affinities, as well as a potential structure, mutagenesis studies will be pursued to try and disrupt the binding interface between the Trf proteins and Mtr4. If successful, then further *in vivo* work will be done with our collaborators in the Ambro van Hoof lab to analyze the effects on RNA surveillance when TRAMP complex formation is disrupted.

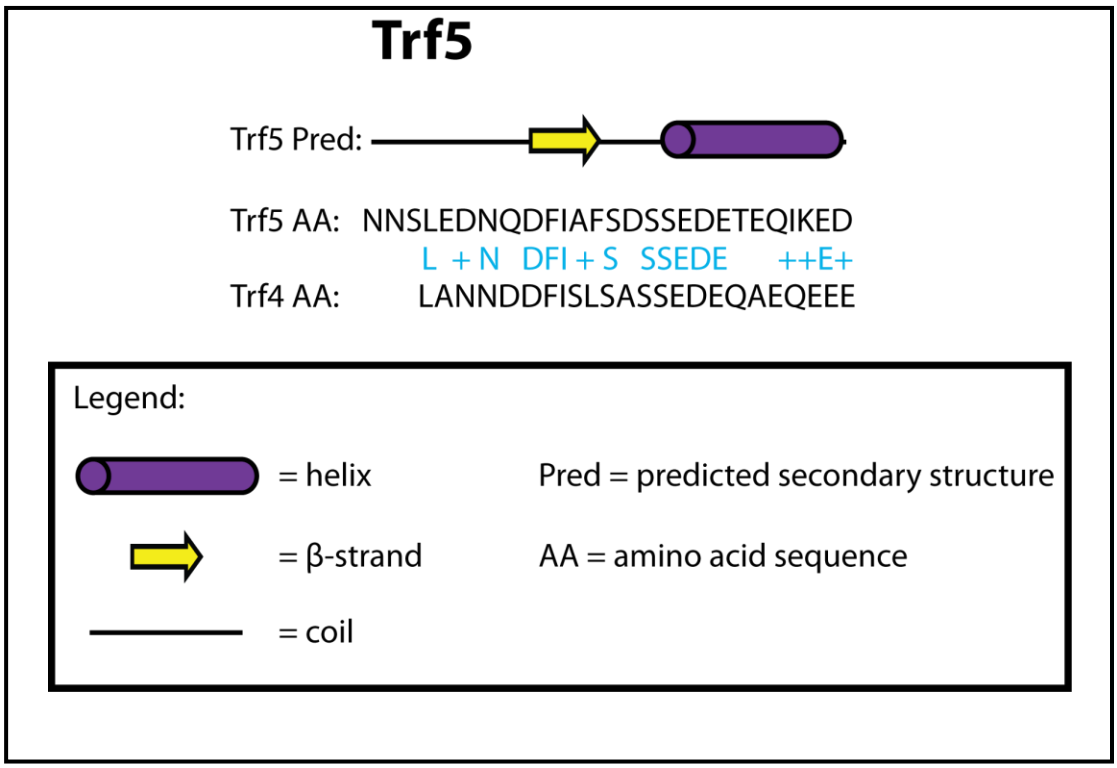

Figure 4-2. Secondary structure prediction of the Trf5 peptide and homologous Trf4 peptide. Above shows a sequence alignment between Trf5 and Trf4, with a secondary structure prediction of Trf5 aligned to the sequences; 50% sequence identity and 71% sequence similarity.

CRYSTALLIZATION TRIALS WITH COMPLEXES

Certain criteria must be met before setting up crystal trays with complexes. When dealing with protein-protein complexes, issues arise all throughout the purification process, from proper buffers and purification methods that keep complexes together, to obtaining greater than 95% purity for crystallization trials. The target criteria used for crystallography grade complex purification is as follows: homogeneity, confirmation of binding (anisotropy, sizing, etc), greater than 95% purity, and greater than 5 mg/ml concentrated protein. When dealing with RNA-protein complexes, RNA is purified separately before mixing with protein in a 2:1 excess of RNA to protein. For Mtr4 crystallization with RNA, attempts have been tried with a non-hydrolyzable ATP analog (AMP-PNP). However, even though the Conti lab

got a crystal structure of Mtr4 bound to RNA with an ATP analog, the Toth lab has shown that the presence of nucleotide decreases Mtr4's RNA binding affinity. Future attempts will not include the presence of an additional nucleotide when trying to crystallize Mtr4 bound to RNA. After all the criteria have been met, crystallization screens can be set-up using our Gryphon robot for 96-well plate crystal trays. Using a variety of commercial screens such as Hampton, Emerald, Jena Bioscience, Qiagen, and Microlytic, as well as the additional variables with three different temperature controlled rooms (4ºC, 13ºC, and room temperature) increases our probability of obtaining crystals.

TRF4-AIR2-MTR4 MUTANTS AND POLY(A) ADDITION

The Jankowsky lab showed E947, a residue that is in close proximity to the bases of the RNA substrate in the crystal structure, to be important for regulating the poly(A) tail addition by Trf4 on RNA substrates[37]. The mutations we have characterized on the ratchet helix are in close proximity to E947, and have been shown to be important in RNA unwinding and substrate specificity. Perhaps these mutations could also be involved in modulating Trf4 addition of a poly(A) tail to the 3' end of substrates. To test this we would need to use a large gel apparatus, which we already have, to be able to distinguish between a single nucleotide in size. We have previously tested polyadenylation activity of Trf4-Air2 in the presence of Rrp6 and have shown poly(A) tail addition. Assays would be set-up in much the same way as the Jankowsky lab has reported, using a 5'- ^{32}P labeled RNA strand[36]. The Mtr4 mutants would have to additionally include the D/E mutation (that eliminates unwinding activity) to allow for monitoring of polyadenylation exclusively.

ARCH MOVEMENT STUDIES

The arch domain of Mtr4 is poorly characterized. The only known function of the arch is RNA binding and the potential for influencing unwinding. The arch displays mobility

based observed conformational changes in the two crystal structures.[27,28] Monitoring movement in the arch could give insight into the different interactions of Mtr4 and how they are initiated. FRET would allow for measurements between the arch domain and a reference point, perhaps, on a close residue located in the core of Mtr4 (needs to be within a distance 10 Å at any given point). With FRET, there is the issue of labeling two cysteines on the same protein (one on the fist, one on domain 2 within 10 Å of the other) with different tags. An existing method addresses this issue by expressing the protein in truncations separately, labeling both fragments separately, and then covalently attaching them by initiating a self-cleaving peptide (intein) that is attached at the N-terminus and C-terminus of the fragmented protein.[83] Another method capable of measuring arch movement is "Double electron-electron resonance" (DEER) spectroscopy. DEER spectroscopy has the capability to measure between paramagnetic centers from 1.5-8 nm, using a tetrazolium compound (MTS) modified residue as the spin label. This approach represents another avenue for future research into arch movement.

SUMMARY

Extensive characterization of the essential RNA helicase Mtr4, was carried out in this thesis work. Residues along the ratchet helix of Mtr4 were characterized and shown to effect unwinding rates; E1033A increased unwinding rates, and R1030A decreased unwinding rates. Furthermore, the R1030A ratchet helix mutant showed no unwinding preference between a poly(A) and non(A) substrate. This is the first identification of a residue of Mtr4 involved in substrate specificity. However, TRAMP (with the R1030A mutation) unwinding rates regain substrate specificity for which we hypothesize that Trf4 and Air2 somehow increase Mtr4's affinity for substrates and/or induce a spatial adaptation in Mtr4 allowing for substrate recognition. Additionally, the arch domain proved to be involved in unwinding, despite previous results suggesting otherwise. Archless-Mtr4 alone has no effect on

unwinding rates, however archless-Mtr4 combined with one of the ratchet helix point mutants (R1030A or E1033A) abolishes unwinding activity. The arch appears to cooperate with the ratchet helix of Mtr4 in unwinding structured RNA. The research presented in this thesis provides valuable insight into unwinding and substrate recognition by Mtr4. Moreover, continuing Mtr4 mutational studies in a TRAMP context and understanding the effects Trf4/5 and Air1/2 have on Mtr4 function would be extremely informative. Further characterization is needed to elucidate the full mechanistic detail, through structural and mutational analysis. This work proves as a solid basis of research creating a foundation for future studies of Mtr4.

REFERENCES

1. Serganov, A. (2009). The long and the short of riboswitches. *Current Opinion in Structural Biology, 19,* 251-259.

2. Choi, S.I., Lim, K., and Seong, B.L. (2011). Chaperoning roles of macromolecules interacting with proteins *in vivo.* International Journal of Molecular Sciences, 12, 1979-1990.

3. Collins, L.J., and Penny, D. (2009). The RNA infrastructure: dark matter of the eukaryotic cell? Trends in Genetics, 25, 120-128.

4. Bernstein, J., and Toth, E.A. (2012). Yeast nuclear RNA processing. World Journal of Biological Chemistry, 3, 7-26.

5. Tollervey, J.R., and Lunyak V.V. (2012). Epigenetics: Judge, jury and executioner of stem cell fate. Epigenetics, 7, 823-840.

6. Allmang, C., Petfalski, E., Podtelejnikov, A., Mann, M., Tollervey, D. and Mitchell, P. (1999) The yeast exosome and human PM-Scl are related complexes of 3'-5' exonucleases. Genes & Development, 13, 2148-2158.

7. Lykke-Andersen, S., Tomecki, R., Jensen, T.H. and Dziembowski, A. (2011). The eukaryotic RNA exosome: same scaffold but variable catalytic subunits. RNA biology, 8, 61-66.

8. Mitchell, P., Petfalski, E., Shevchenko, A., Mann, M. and Tollervey, D. (1997) The exosome: a conserved eukaryotic RNA processing complex containing multiple 3'-5' exoribonucleases. Cell, 91, 457-466.

9. Wolin, S.L., Sim, S. and Chen, X. (2012) Nuclear noncoding RNA surveillance: is the end in sight? Trends in Genetics, 28, 306-313.

10. Jensen, T.B. (2010) RNA Exosome. Landes Bioscience, Austin, TX.

11. Liu, Q., Greimann, J.C., and Lima, C.D. (2006). Reconstitution, Activities, and Structure of the Eukaryotic RNA Exosome. Cell, 127, 1223-1237.

12. Wasmuth, E.V., and Lima, C.D. (2012). Exo- and Endoribonucleolytic Activities of Yeast Cytoplasmic and Nuclear RNA Exosomes Are Dependent on the Noncatalytic Core and Central Channel. Molecular Cell, 10, 1016.

13. Lee, G., Bratkowski, M.A., Ding, F., Ke, A., and Ha, T. (2012). Elastic Coupling Between RNA Degradation and Unwinding by an Exoribonuclease. Science, 336, 1726.

14. Januszyk, K., Liu, Q., and Lima, C.D. (2011). Activities of human RRP6 and structure of the human RRP6 catalytic domain. RNA Biology, 17(8), 1566-1577.

15. Stead, J.A., Costello, J.L., Livingstone, M.J., and Mitchel, P. (2007). The PMC2NT domain of the catalytic exosome subunit Rrp6p provides the interface for binding with its cofactor Rrp47p, a nucleic acid-binding protein. Nucleic Acids Research, 35(16), 5556-5567.

16. Callahan, K.P., and Butler, J.S. (2009). TRAMP Complex Enhances RNA Degradation by the Nuclear Exosome Component Rrp6. The Journal of Biological Chemistry, 285, 3540-3547.

17. Callahan, K.P., and Butler, J.S. (2008). Evidence for core exosome independent function of the nuclear exoribonuclease Rrp6p. Nucleic Acids Research, 36(21), 6645-6655.

18. Butler, J.S., and Mitchell, P. (2010). Rrp6, Rrp47 and cofactors of the nuclear exosome. Advances in Experimental Medicine and Biology, 702, 91-104.

19. Holub, P., Lalakova, J., Cerna, H., Pasulka, J., Sarazova, M., Hrazdilova, K., Arce, M.S., Hobor, F., Stefl, R., and Vanacova, S. (2012). Air2p is critical for the assembly and RNA-binding of the TRAMP complex and the KOW domain of Mtr4p is crucial for exosome activation. Nucleic Acids Research, 40(12), 5679-5693.

20. Bernstein, J., Patterson, D.N., Wilson, G.M., and Toth, E.A. (2008). Characterization of the essential activities of Saccharomyces cerevisiae Mtr4p, a 3'-5' helicase partner of the nuclear exosome. Journal of Biological Chemistry, 283(8), 4930-4942.

21. Hardwick, S.W., and Luisi, B.F. (2013). RNA helicases and their busy contributions to RNA degradation, regulation and quality control. RNA biology, 10(1), 56-70.

22. Johnson, S.J., and Jackson, R.N. (2012). Ski2-like RNA helicase structures: Common themes and complex assemblies. RNA biology, 10.

23. Ye, J., Osborne, A.R., Groll, M., and Rapoport, T.A. (2004). RecA-like motor ATPases—lessons from structures. Biochimica et Biophysica Acta, 1659, 1-18.

24. Deng, X., Habel, J.E., Kabaleeswaran, V., Snell, E.H., Wold, M.S., and Borgstahl, G.E. (2007). Structure of the full-length human RPA14/32 complex gives insight into the mechanism of DNA binding and complex formation. Journal of molecular biology, 374, 865-876.

25. Woodman, I.L., and Bolt, E.L. (2011). Winged helix domains with unknown function in Hel308 and related helicases. Biochemical Society Transactions, 39, 140-144.

26. Büttner, K., Nehring, S., and Hopfner, K.P. (2007). Structural basis for DNA duplex separation by a superfamily-2 helicase. Nature Structural and Molecular Biology, 14(7), 647-652.

27. Jackson, R.N., Klauer, A.A., Hintze, B.J., Robinson, H., van Hoof, A., and Johnson, S.J. (2010). The crystal structure of Mtr4 reveals a novel arch domain required for rRNA processing. The EMBO Journal, 29, 2205-2216.

28. Weir, J.R., Bonneau, F., Hentschel, J. and Conti, E. (2010) Structural analysis reveals the characteristic features of Mtr4, a DExH helicase involved in nuclear RNA processing and surveillance. Proceedings of the National Academy of Sciences of the United States of America, 107, 12139-12144.

29. Klauer, A.A., and van Hoof, A. (2013). Genetic interactions suggest multiple distinct roles of the arch and core helicase domains of Mtr4 in Rrp6 and exosome function. Nucleic Acids Research, 41(1), 533-541.

30. Jankowsky, E. (2010) RNA Helicases. Cambridge, UK: Royal Society of Chemistry.

31. Bernstein, J., Ballin, J.D., Patterson, D.N., Wilson, G.M., and Toth, E.A. (2010). Unique Properties of the Mtr4p-Poly(A) Complex Suggest a Role in Substrate Targeting. Biochemistry, 49, 10357-10370.

32. Bernstein, J., and Toth, E.A. (2012). Yeast nuclear RNA processing. World Journal of Biological Chemistry, 3, 7-26.

33. Wlotzka, W., Kudla, G., Granneman, S., and Tollervey, D. (2011). The nuclear RNA polymerase II surveillance system targets polymerase III transcripts. The EMBO Journal, 30(9), 1790-1803.

34. Jia, H., Wang, X., Liu, F., Guenther, U., Srinivasan, S., Anderson, J., and Jankowsky, E. (2011). The RNA Helicase Mtr4p Modulates Polyadenylation in the TRAMP Complex. *Cell, 145,* 890-901.

35. LaCava, J., Houseley, J., Saveanu, C., Petfalski, E., Thompson, E., Jacquier, A., and Tollervey, D. (2005). RNA degradation by the exosome is promoted by a nuclear polyadenylation complex. Cell, 121, 713-724.

36. Jia, H., Wang, X., Liu, F., Guenther, U.P., Srinivasan, S., Anderson, J.T., and Jankowsky, E. (2011). The RNA helicase Mtr4p modulates polyadenylation in the TRAMP complex. Cell, 145(6), 890-901.

37. Jia, H., Wang, X., Anderson, J.T., and Jankowsky, E. (2012). RNA unwinding by the Trf4/Air2/Mtr4 polyadenylation (TRAMP) complex. Proceedings of the National Academy of Sciences of the United States of America, 109(19), 7292-7297.

38. Bernstein, J. and Toth, E.A. (2012) Yeast nuclear RNA processing. World Journal of Biological Chemistry, 3, 7-26.

39. Lebreton, A. and Seraphin, B. (2008) Exosome-mediated quality control: substrate recruitment and molecular activity. Biochimica et Biophysica Acta, 1779, 558-565.

40. Ibrahim, H., Wilusz, J. and Wilusz, C.J. (2008) RNA recognition by 3'-to-5' exonucleases: the substrate perspective. Biochimica et Biophysica Acta, 1779, 256-265.

41. Astuti, D., Morris, M.R., Cooper, W.N., Staals, R.H., Wake, N.C., Fews, G.A., Gill, H., Gentle, D., Shuib, S., and Ricketts, C.J. (2012) Germline mutations in DIS3L2 cause the Perlman syndrome of overgrowth and Wilms tumor susceptibility. Nature Genetics, 44, 277-284.

42. Bruserud, O. (2007) Introduction: RNA and the treatment of human cancer. Current Pharmaceutical Biotechnology, 8, 318-319.

43. Fabre, A., Charroux, B., Martinez-Vinson, C., Roquelaure, B., Odul, E., Sayar, E., Smith, H., Colomb, V., Andre, N., and Hugot, J.P. (2012) SKIV2L mutations cause syndromic diarrhea, or trichohepatoenteric syndrome. American Journal of Human Genetics, 90, 689-692.

44. Nelson, P.T. and Keller, J.N. (2007) RNA in brain disease: no longer just "the messenger in the middle". Journal of Neuropathology and Experimental Neurology, 66, 461-468.

45. Staals, R.H. and Pruijn, G.J. (2011) The human exosome and disease. Advances in Experimental Medicine and Biology, 702, 132-142.

46. Allmang, C., Petfalski, E., Podtelejnikov, A., Mann, M., Tollervey, D. and Mitchell, P. (1999) The yeast exosome and human PM-Scl are related complexes of 3' --> 5' exonucleases. Genes & Development, 13, 2148-2158.

47. Lykke-Andersen, S., Tomecki, R., Jensen, T.H. and Dziembowski, A. (2011) The eukaryotic RNA exosome: same scaffold but variable catalytic subunits. RNA Biology, 8, 61-66.

48. Mitchell, P., Petfalski, E., Shevchenko, A., Mann, M. and Tollervey, D. (1997) The exosome: a conserved eukaryotic RNA processing complex containing multiple 3'-->5' exoribonucleases. Cell, 91, 457-466.

49. LaCava, J., Houseley, J., Saveanu, C., Petfalski, E., Thompson, E., Jacquier, A. and Tollervey, D. (2005) RNA degradation by the exosome is promoted by a nuclear polyadenylation complex. Cell, 121, 713-724.

50. Vanacova, S., Wolf, J., Martin, G., Blank, D., Dettwiler, S., Friedlein, A., Langen, H., Keith, G. and Keller, W. (2005) A new yeast poly(A) polymerase complex involved in RNA quality control. PLoS Biology, 3, e189.

51. Wyers, F., Rougemaille, M., Badis, G., Rousselle, J.C., Dufour, M.E., Boulay, J., Regnault, B., Devaux, F., Namane, A., and Seraphin, B. (2005) Cryptic pol II transcripts are degraded by a nuclear quality control pathway involving a new poly(A) polymerase. Cell, 121, 725-737.

52. Anderson, J.T. and Wang, X. (2009) Nuclear RNA surveillance: no sign of substrates tailing off. Critical Reviews in Biochemistry and Molecular Biology, 44, 16-24.

53. Bayne, E.H., White, S.A. and Allshire, R.C. (2007) DegrAAAded into silence. Cell, 129, 651-653.

54. Houseley, J. and Tollervey, D. (2009) The many pathways of RNA degradation. Cell, 136, 763-776.

55. Vanacova, S. and Stefl, R. (2007) The exosome and RNA quality control in the nucleus. EMBO Reports, 8, 651-657.

56. Buhler, M., Haas, W., Gygi, S.P. and Moazed, D. (2007) RNAi-dependent and -independent RNA turnover mechanisms contribute to heterochromatic gene silencing. Cell, 129, 707-721.

57. Houseley, J., Kotovic, K., El Hage, A. and Tollervey, D. (2007) Trf4 targets ncRNAs from telomeric and rDNA spacer regions and functions in rDNA copy number control. The EMBO Journal, 26, 4996-5006.

58. Wang, S.W., Stevenson, A.L., Kearsey, S.E., Watt, S. and Bahler, J. (2008) Global role for polyadenylation-assisted nuclear RNA degradation in posttranscriptional gene silencing. Molecular and Cellular Biology, 28, 656-665.

59. Lykke-Andersen, S., Brodersen, D.E. and Jensen, T.H. (2009) Origins and activities of the eukaryotic exosome. Journal of Cell Science, 122, 1487-1494.

60. Lin-Chao, S., Chiou, N.T. and Schuster, G. (2007) The PNPase, exosome and RNA helicases as the building components of evolutionarily-conserved RNA degradation machines. Journal of Biomedical Science, 14, 523-532.

61. Liang, S., Hitomi, M., Hu, Y.H., Liu, Y. and Tartakoff, A.M. (1996) A DEAD-box-family protein is required for nucleocytoplasmic transport of yeast mRNA. Molecular and Cellular Biology, 16, 5139-5146.

62. van Hoof, A., Lennertz, P. and Parker, R. (2000) Yeast exosome mutants accumulate 3'-extended polyadenylated forms of U4 small nuclear RNA and small nucleolar RNAs. Molecular and Cellular Biology, 20, 441-452.

63. Buttner, K., Nehring, S. and Hopfner, K.P. (2007) Structural basis for DNA duplex separation by a superfamily-2 helicase. Nature Structural & Molecular Biology, 14, 647-652.

64. Halbach, F., Rode, M. and Conti, E. (2012) The crystal structure of S. cerevisiae Ski2, a DExH helicase associated with the cytoplasmic functions of the exosome. RNA, 18, 124-134.

65. He, Y., Andersen, G.R. and Nielsen, K.H. (2011) Structural basis for the function of DEAH helicases. EMBO Reports, 11, 180-186.

66. Oyama, T., Oka, H., Mayanagi, K., Shirai, T., Matoba, K., Fujikane, R., Ishino, Y. and Morikawa, K. (2009) Atomic structures and functional implications of the archaeal RecQ-like helicase Hjm. BMC Structural Biology, 9, 2.

67. Richards, J.D., Johnson, K.A., Liu, H., McRobbie, A.M., McMahon, S., Oke, M., Carter, L., Naismith, J.H. and White, M.F. (2008) Structure of the DNA repair helicase hel308 reveals DNA binding and autoinhibitory domains. The Journal of Biological Chemistry, 283, 5118-5126.

68. Walbott, H., Mouffok, S., Capeyrou, R., Lebaron, S., Humbert, O., van Tilbeurgh, H., Henry, Y. and Leulliot, N. (2010) Prp43p contains a processive helicase structural architecture with a specific regulatory domain. The EMBO Journal, 29, 2194-2204.

69. Zhang, X., Nakashima, T., Kakuta, Y., Yao, M., Tanaka, I. and Kimura, M. (2008) Crystal structure of an archaeal Ski2p-like protein from Pyrococcus horikoshii OT3. Protein Science, 17, 136-145.

70. Pena, V., Jovin, S.M., Fabrizio, P., Orlowski, J., Bujnicki, J.M., Luhrmann, R. and Wahl, M.C. (2009) Common design principles in the spliceosomal RNA helicase Brr2 and in the Hel308 DNA helicase. Molecular Cell, 35, 454-466.

71. Zhang, L., Xu, T., Maeder, C., Bud, L.O., Shanks, J., Nix, J., Guthrie, C., Pleiss, J.A. and Zhao, R. (2009) Structural evidence for consecutive Hel308-like modules in the spliceosomal ATPase Brr2. Nature Structural & Molecular Biology, 16, 731-739.

72. Singleton, M.R., Dillingham, M.S. and Wigley, D.B. (2007) Structure and mechanism of helicases and nucleic acid translocases. Annual Review of Biochemistry, 76, 23-50.

73. Small, E.C., Leggett, S.R., Winans, A.A. and Staley, J.P. (2006) The EF-G-like GTPase Snu114p regulates spliceosome dynamics mediated by Brr2p, a DExD/H box ATPase. Molecular Cell, 23, 389-399.

74. Holm, L. and Rosenstrom, P. (2010) Dali server: conservation mapping in 3D. Nucleic Acids Research, 38, W545-549.

75. Larkin, M.A., Blackshields, G., Brown, N.P., Chenna, R., McGettigan, P.A., McWilliam, H., Valentin, F., Wallace, I.M., Wilm, A., and Lopez, R. (2007) Clustal W and Clustal X version 2.0. Bioinformatics (Oxford, England), 23, 2947-2948.

76. Ashkenazy, H., Erez, E., Martz, E., Pupko, T. and Ben-Tal, N. (2010) ConSurf 2010: calculating evolutionary conservation in sequence and structure of proteins and nucleic acids. Nucleic acids research, 38, W529-533.

77. Wang, X., Jia, H., Jankowsky, E. and Anderson, J.T. (2008) Degradation of hypomodified tRNA(iMet) in vivo involves RNA-dependent ATPase activity of the DExH helicase Mtr4p. RNA, 14, 107-116.

78. Sikorski, R.S. and Hieter, P. (1989) A system of shuttle vectors and yeast host strains designed for efficient manipulation of DNA in Saccharomyces cerevisiae. Genetics, 122, 19-27.

79. Cordin, O., Hahn, D. and Beggs, J.D. (2012) Structure, function and regulation of spliceosomal RNA helicases. Current Opinion in Cell Biology, 24, 431-438.

80. Yang, Q. and Jankowsky, E. (2005) ATP- and ADP-dependent modulation of RNA unwinding and strand annealing activities by the DEAD-box protein DED1. Biochemistry, 44, 13591-13601.

81. Ponting, C.P. (2000) Proteins of the endoplasmic-reticulum-associated degradation pathway: domain detection and function prediction. The Biochemical Journal, 351, 527-535.

82. Wagner, J.D.O., Jankowsky, E., Company, M., Pyle, A.M., and Abelson, J.N. (1998) The DEAH-box protein PRP22 is an ATPase that mediates ATP-dependent mRNA release from the spliceosome and unwinds RNA duplexes. The EMBO Journal, 17(10), 2926-2937.

83. Yang, J.Y., and Yang, W.Y. (2009) Site-specific two-color protein labeling for FRET studies using split inteins. J. of the Am. Chem. Soc., 131, 11644-11645.